KINETICS OF NATURAL ORGANIC MATTER AS THE INITIATOR, PROMOTER AND INHIBITOR IN WATER OZONATION AND ITS INFLUENCES ON THE REMOVAL OF IBUPROFEN

YONG EE LING

(M. Eng., Universiti Teknologi Malaysia)

A THESIS SUBMITTED

FOR THE DEGREE OF DOCTOR OF PHILOSOPHY

DEPARTMENT OF CIVIL AND ENVIRONMENTAL ENGINEERING

NATIONAL UNIVERSITY OF SINGAPORE

2012

DECLARATION

I hereby declare that this thesis is my original work and it has been written by me in its entirety. I have duly acknowledged all the sources of information which have been used in the thesis.

This thesis has also not been submitted for any degree in any university previously.

_____

Yong Ee Ling

3 August 2012

ACKNOWLEDGEMENT

"Thank you" would not be enough to express my deepest gratitude to thank the kind Samaritans who have made this doctoral thesis possible in various ways.

First and foremost, I owe my sincere and earnest thankfulness to my respectable supervisor, Assistant Professor Dr. Lin Yi-Pin, who has been patient, supportive and helpful in dealing with my many shortcomings. Without his strong and immense knowledge in environmental chemistry, the fundamental study in the field of water ozonation would not have been successful. His good and critical advices have been invaluable on both an academic and a personal level, for which I am extremely grateful. I am truly indebted and thankful for the financial support Dr. Lin has provided me via research grant for the past two years which allowed me to continue my study without any financial difficulties.

It also gives me great pleasure to thank Professor Liu Wen-Tso, currently a faculty in University of Illinois, Urbana Champaign, for giving me the opportunity to join NUS during his service here. My gratitude is extended to the faculty members of NUS who has involved in both comprehensive and oral qualifying exam, particularly Associate Professor Dr. Bai Renbi, Associate Professor Dr. Balasubramanian Rajasekhar, Associate Professor He Jianzhong, Associate Professor Paul Chen Jia-Ping and Associate Professor Yu Liya for their critical but kind evaluation. I would like to thank all the laboratory staffs in the Department of Civil and Environmental Engineering (Temasek and Water Science & Technology laboratories), especially Mr. Micheal Tan Eng Hin, Mdm. Susan Chia, Mdm. Tan Hwee Bee, Mr. Sukiantor bin Tokiman, Mr. Mohamed Sidek bin Ahmad, Mr Chandrasegaran S/O Govindaraju and Mdm. Tan Xiaolan for their generous help in creating a safe and conducive working

environment, not forgetting Ms. Hannah Foong who has been a great management officer (previously in Division of Environmental Science and Engineering) and friend. I also would like to acknowledge the financial, academic and technical support provided by National University of Singapore and its staffs, specifically NUS Research Scholarship and NUS FRC Grant that provided necessary funding for me and this research, respectively. The library and computer facilities of the university have been indispensable.

I am obliged to many of my buddies (Dr. Yang Lei, Mr. Ng Ding Quan, Ms. Zhang Yuanyuan, Dr. Lee Lai Yoke, Dr. Guo Huiling, Dr. Hong Peiying, Dr. Albert Ng Tze Chiang, Dr. Yang Liming, Ms. Nichanan Thepsuparungsikul, Dr. Suresh Kumar Balasubramanian, Ms. Low Siok Ling and Dr. Zhang Linzi) who have given me invaluable encouragement throughout.

A great honor should go to my beloved parents who have loved and supported me unconditionally throughout their life. I sincerely express a heartfelt gratitude to my elder sister and younger brother who have been shouldering all the family responsibilities which enabled me to pursue my studies without worries. Last but not least, I owe my loving thanks to my husband for being considerate and cheerful even when I was being difficult.

To all the good Samaritans who have involved, may:

"the Lord bless you and keep you,

the Lord make his face shine on you and be gracious to you,

the Lord turn his face toward you and give you peace."

– Numbers 6:24-26

TABLE OF CONTENT

SUMMARY

Natural organic matter (NOM) can simultaneously react as the initiator, promoter and inhibitor in hydroxyl radical (·OH) chain reactions in water ozonation. The rate constants of NOM in these reactions, however, have never been quantified due to their complexity. This results in difficulties to quantitatively describe the influences of NOM on the degradation of organic pollutants, such as pharmaceutical compounds, by ozonation. The aims of this study were to develop a new method to quantify these different reaction rate constants of NOM in water ozonation and to study their influences on the removal of ibuprofen, a commonly detected pharmaceutical compound in surface water.

In this study, a new method integrating the transient steady-state ·OH model, the R_{ct} concept and the pseudo first-order ozone decomposition model that can be used to determine the different rate constants of NOM was developed. With the addition of an external inhibitor (*tert*-butanol), the rate constants of NOM as the initiator and inhibitor can be determined from the slope and intercept of the plot of $1/R_{ct}$ vs. the external inhibition capacity, respectively. The rate constant of NOM as the promoter can be determined from the slope of the plot of pseudo first-order ozone decomposition rate constant vs. the R_{ct}. This method was first validated using simple model compounds that are representative of the initiator, promoter and inhibitor followed by its applications to three NOM isolates and a natural water.

The determined rate constants of NOM were used to quantitatively describe the influences of NOM on the removal of ibuprofen in the presence of carbonate alkalinity. The experimental results and model simulation revealed that the presence of NOM generally enhanced the removal of ibuprofen, which was simultaneously

influenced by the ozone exposure, OH^- initiation capacity (or pH value), NOM initiation and inhibition capacities, and carbonate alkalinity inhibition capacity.

LIST OF TABLES

LIST OF FIGURES

CHAPTER 1

INTRODUCTION AND BACKGROUND

1.1 Ozonation of organic compounds

The use of ozone in advanced drinking water treatment has become popular since the 1970s [1-3]. It has been widely used for the inactivation of pathogens [4-8] and oxidation of organic pollutants [9-12]. Ozone decomposes in pure water via its reaction with the hydroxide ion (OH^-) [13, 14], leading to the formation of superoxide radical ($\cdot O_2^-$) and subsequently hydroxyl radical (OH) through a series of chain reactions [15-17]. Thus, the removal of organic contaminants in ozonation can proceed in two reaction pathways: direct reactions involving ozone molecules and free radical reactions involving ·OH [18].

Direct ozone reaction is highly selective. It targets the electron rich region of organic molecules, such as the carbon-carbon double bond [18]. The second order rate constants for ozone direct reactions range from 0.003 $M^{-1}s^{-1}$ to 10^5 $M^{-1}s^{-1}$ [19]. On the other hand, the ·OH reactions is non-selective with second order rate constants ranging from 10^7 $M^{-1}s^{-1}$ to 10^{10} $M^{-1}s^{-1}$ [20-23]. The ·OH attacks organic molecules via two pathways: the radical addition or the hydrogen abstraction [24, 25]. In the former, the ·OH is added to an unsaturated aliphatic or aromatic compound and produces an organic radical that can further react with oxygen to produce stable oxidized end products. In the latter, hydrogen atom is removed from organic compound to form a radical that reacts with oxygen to produce a peroxyl radical.

A schematic diagram representing the ozone chain reactions in the presence of foreign compounds is illustrated in Figure 1.1 [26]. Depending on the “net” formation

or consumption of ·OH, these foreign compounds can be classified as the initiator, promoter or inhibitor based on the following definitions [26]:

a. Initiators: compounds that react directly with ozone forming $\cdot O_3^-$, which subsequently converts to ·OH via chain reactions.
b. Promoters: compounds that react with ·OH and propagate the radical chain to ultimately produce another ·OH. There is no net ·OH production or consumption.
c. Inhibitors: compounds that react with the ·OH and terminate the chain reaction.

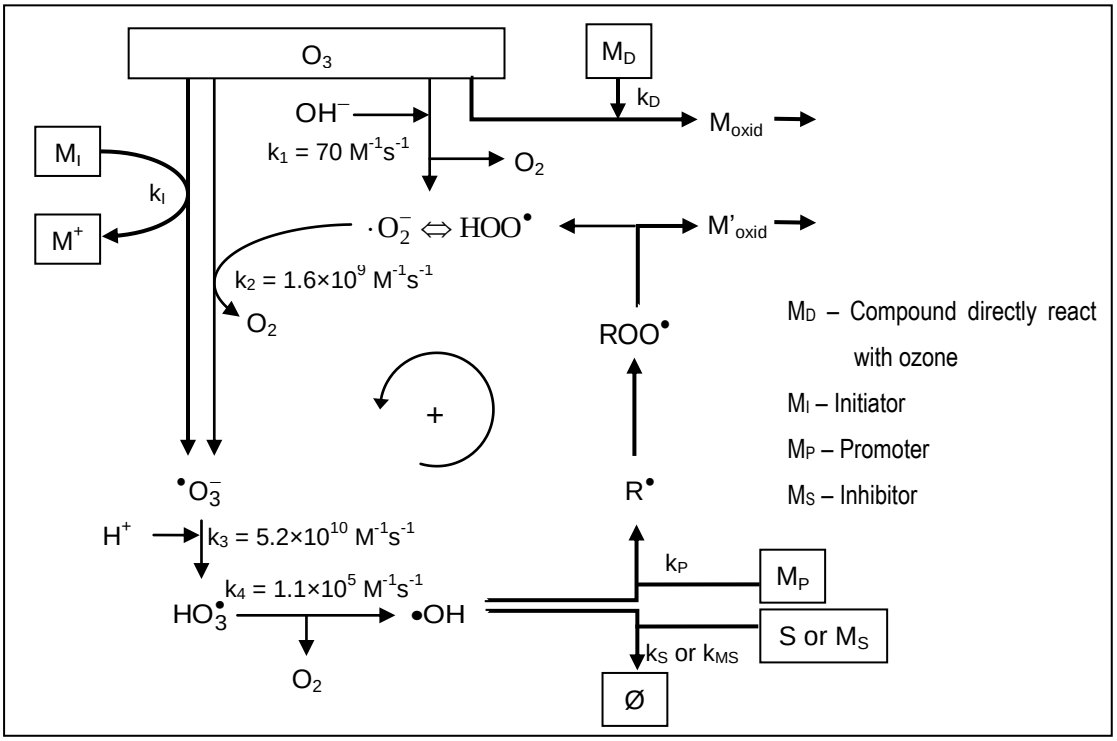

Figure 1.1 Reactions of ozone with the presence of foreign compounds acting as the initiator, promoter and inhibitor [26]

Considering all reactions leading to the decomposition of ozone and assuming that all the radicals in the chain reactions are at steady state, the decomposition of ozone can be described by a pseudo first-order kinetic as shown in Equation (1.1)

$$
\begin{aligned}
&-\frac{d[O_3]}{dt}\frac{1}{[O_3]} = k_{obs} \\
&= k_1[OH^-] + \sum(k_{D,i}[M_{D,i}]) + \{2k_1[OH^-] + \sum(k_{I,i}[M_{I,i}])\}\left(1 + \frac{\sum(k_{P,i}[M_{P,i}])}{\sum(k_{S,i}[M_{S,i}])}\right) \\
&= 3k_1[OH^-] + \sum(k_{D,i}[M_{D,i}]) + \sum(k_{I,i}[M_{I,i}]) + \sum(k_{P,i}[M_{P,i}])\left(\frac{2k_1[OH^-] + \sum(k_{I,i}[M_{I,i}])}{\sum(k_{S,i}[M_{S,i}])}\right)
\end{aligned}
\tag{1.1}
$$

where $[O_3]$ is the ozone concentration; k_{obs} represents the pseudo first-order rate constant of O_3 decomposition; k_1 represents the reaction rate constant between OH^- and ozone; $M_{D,i}$ represents the compound that directly reacts with ozone; $M_{I,i}$ represents the initiator; $M_{P,i}$ represents the promoter; $M_{S,i}$ represents the inhibitor; $k_{D,i}$, $k_{I,i}$, $k_{P,i}$ and $k_{S,i}$ represents rate constants for direct ozone reaction, initiation, promotion and inhibition reactions, respectively.

The concentration of ·OH is at a transient steady-state and can be expressed by the following equations [26]:

$$
[\cdot OH] = \frac{2k_1[OH^-] + \sum k_{I,i}[M_{I,i}]}{\sum k_{S,i}[M_{S,i}]}[O_3] \tag{1.2}
$$

where [·OH] is the transient steady-state ·OH concentration.

Depending on the nature of the foreign compound, it can react solely as the initiator, promoter, inhibitor, or simultaneously as any combination of these modes. For example, *tert*-butanol and acetate can react as an inhibitor to decrease the ozone decomposition by scavenging the OH [26, 27]. Meanwhile, complex molecules such as natural organic matter can be the initiator, promoter and inhibitor simultaneously [26, 28].

1.2 The R_{ct} concept

In water ozonation, it is difficult to directly measure the ·OH concentration due to its extremely low steady-state concentrations ($\leq 10^{-12}$ M) and fast reaction kinetics [27, 29]. Thus, it is common to utilize a probe compound to determine its kinetic behavior. The probe compound that is widely used is *ρ*-chlorobenzoic acid (pCBA) [27, 30-32]. It is selected due to its low reactivity with ozone ($k_{O_3/pCBA} \leq 0.15$ $M^{-1}s^{-1}$ [33]), but high reactivity with ·OH ($k_{\cdot OH/pCBA} = 5\times10^9$ $M^{-1}s^{-1}$ [34]). Employing pCBA as a probe compound creates competition reactions between pCBA and the target compound (M) for ·OH as described below:

$$\cdot OH + M \rightarrow product \quad (1.3)$$

$$\cdot OH + pCBA \rightarrow product \quad (1.4)$$

The decay rates of pCBA and compound M can be described as the following:

$$-\frac{d[pCBA]}{dt} = k_{\cdot OH/pCBA}[\cdot OH][pCBA] \quad (1.5)$$

$$-\frac{d[M]}{dt} = k_{\cdot OH/M}[\cdot OH][M] \quad (1.6)$$

The competition kinetics allows the determination of the unknown rate constant for compound M from the following relationship:

$$\ln\left(\frac{[pCBA]_t}{[pCBA]_0}\right) = \frac{k_{\cdot OH/pCBA}}{k_{\cdot OH/M}} \ln\left(\frac{[M]_t}{[M]_0}\right) \quad (1.7)$$

where $k_{OH/pCBA}$ and $k_{OH/M}$ denote the rate constants of ·OH with pCBA and M, respectively..

Although pCBA serves as an excellent probe compound in monitoring ·OH concentration, an error is likely to occur if more than 5% of the total ·OH scavenging capacity is consumed by pCBA [30]. Therefore, a low concentration of pCBA, typically in the range of 0.25 μM to 0.5 μM, is essential when it is employed to probe the reaction kinetics between ·OH and organic contaminants [27].

To experimentally determine the ·OH exposure of a target compound in water ozonation, the R_{ct} concept, which is defined as the ratio of ·OH exposure to ozone exposure, was developed by Elovitz and von Gunten [27]:

$$R_{ct} = \frac{\int[\cdot OH]dt}{\int[O_3]dt} \quad (1.8)$$

The value of R_{ct} can be determined by following the decay of the probe compound as a function of ozone exposure.

$$\ln\left(\frac{[pCBA]_t}{[pCBA]_0}\right) = -k_{\cdot OH/pCBA} R_{ct} \int [O_3] dt \quad (1.9)$$

The R_{ct} value has been shown to follow a two-stage pattern in the ozonation of natural waters, i.e. an initial stage (< 20 s) with a high R_{ct} value followed by a lower value that remains constant during the course of ozonation [27]. The initial high R_{ct} stage is believed to be caused by the initiation reactions involving the ubiquitously present natural organic matter [35, 36]. As the ozone concentration can be easily measured, the constant R_{ct} value allows the calculation of the ·OH concentration in the second R_{ct} stage of the ozonation process.

The R_{ct} concept is useful and paves a way to model the degradation of pollutants in water ozonation [27]. Recent studies using the quench-flow technique have revealed more details of the initial high R_{ct} stage showing that the high R_{ct} value may vary as a function of time and its value is about 2-3 orders of magnitude greater than that of the second stage [37]. However, the respective effects of initiator, promoter and inhibitor on the R_{ct} value cannot be quantitatively determined. The lack of this insight makes it difficult to quantitatively determine the impacts of compounds that are involved in the ·OH chain reactions on the removal of target pollutants, particularly those reacting as the promoter.

1.3 Natural organic matter (NOM)

NOM consists of refractory organic materials derived from decayed plants/microorganisms and exists ubiquitously in natural waters [38, 39]. As a result, it possesses a variety of different functional groups [40, 41]. Dissolved organic carbon (DOC) is the most-used gross surrogate for NOM.

It is common to fractionate NOM using macroporous, nonionic Amberlite XAD resins [42-44] due to their greater adsorption capacities and relatively easier elution compared to alumina, silica gel, nylon and polyamide powder [45]. These resins also avoid the alteration of the molecular structure of the adsorbed NOM during the elution process [45]. Among the resins, XAD-8 resin is found to favor hydrophobic compounds [46] and has been shown to be able to efficiently concentrate and isolate hydrophobic fraction of NOM in natural waters [47]. The hydrophilic fraction in the effluent of the XAD-8 resin can be adsorbed using XAD-4 resin, which was successfully demonstrated by Aiken *et al.* [44]. A schematic of the fractionation procedures is shown in Figure 1.2. Among those fractions, the hydrophobic fraction, consisting of both humic and fulvic acids, constitutes one-third to one half of the DOC in natural water [43]. Humic and fulvic acids are differentiated by their solubility in acid and base. Humic acid is soluble in base but insoluble in acid (< pH 2) whereas fulvic acid dissolves in both acid and base.

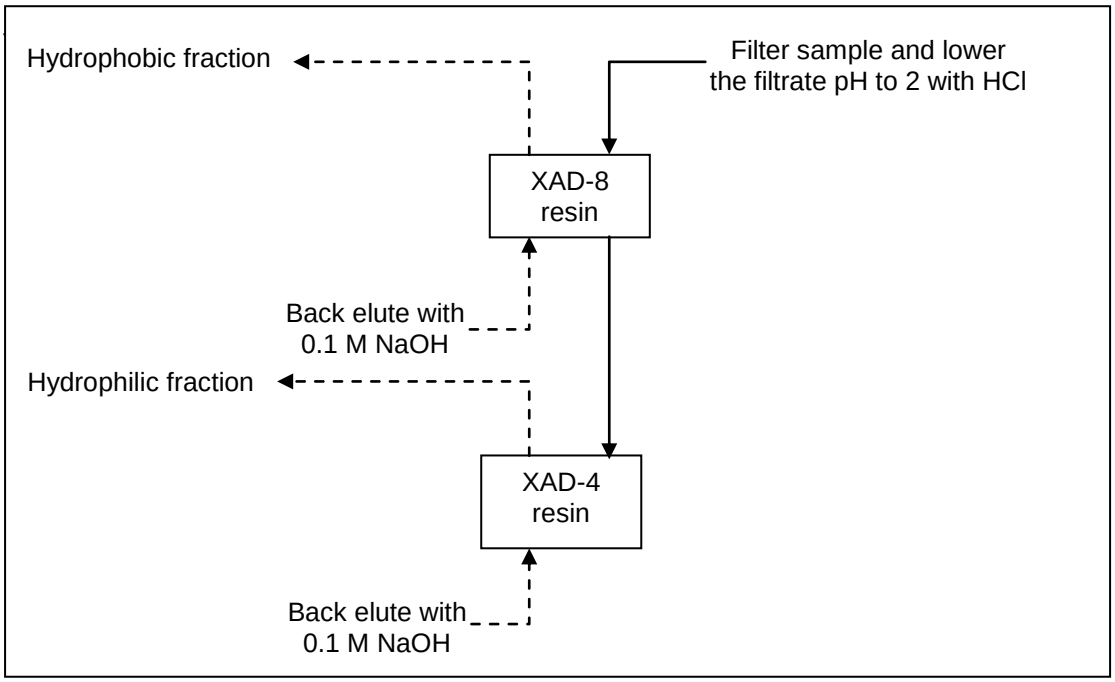

Figure 1.2 Schematic diagram for NOM isolation/fractionation using XAD-8/XAD-4 resins [43, 44]

Table 1.1 presents studies on the isolation and fractionation of NOM present in water taken from different geographical locations. The table shows that the NOM content vary from one water source to another and its concentration, composition and chemistry are highly variable. These properties are dependent on the source of organic matter, seasonal changes, temperature, pH, ionic strength, major cations present, surface chemistry of sediment sorbents and the presence of photolytic and microbiological degradation processes [48, 49]. Krasner *et al.* [48] found that the hydrophobic fraction contained more aromatic compounds, mostly phenol and cresol, with a predominance of fulvic acid over humic acid, whereas the hydrophilic fraction contains more carboxyl functional groups. Characterization of aquatic fulvic and humic acids from different water sources done by Reckhow *et al.* [50] showed that the fulvic acid fraction consists of 14-19% of aromatic carbon with the majority of the carbon in aliphatic chain, whereas the humic acid fraction shows a much larger aromatic content (30-50%) with a lower aliphatic content. Fulvic acid is found to dominate the hydrophobic fractions and its molecular weight is generally lower than humic acid. The typical molecular weight of fulvic acid is less than 2000 daltons and that of humic acids ranges from 2000 to10000 daltons [51].

Table 1.1 Percentage of NOM fractions from different water sources

Sources	Fraction		Reference
	Hydrophobic	**Hydrophilic**	
Surface waters			
Apremont Reservoir (France)	51%	49%	[48]
Central New Jersey WTPs	30 – 40%	60 – 70%	[52]
Suwannee River, Drumond Lake, Newport River and Cypress Swamp	75%-90%	10 – 25%	[53]
Han River, Korea	55 – 70%	30 – 45%	[54, 55]
Underground water			
Mosina Water Intake, Poland	85%	15%	[56]

The complex structures of humic and fulvic acids give them the following chemical features [57]:

a. Polyfunctionality: The presence of a variety of functional groups with a broad range of reactivity that is representative of a heterogeneous mixture of interacting polymers.
b. Macromolecular charge: The presence of an anionic charge in the macromolecular framework.
c. Hydrophilicity: The tendency to form strong hydrogen bonds between the solvating polar functional groups, like carboxyl and phenolic groups, with water molecules.
d. Structural lability: The capacity to associate intermolecularly and to change their molecular conformation in response to the change in pH, redox conditions, electrolyte concentration and binding by surrounding functional groups.

In water treatment, NOM has been a primary target to be removed by many processes because it is the precursor of disinfectant by-products (DBPs) [50, 55, 58] such as trihalomethanes (THMs) and haloacetic acids (HAAs), which are carcinogenic [52, 53, 55, 56]. NOM also causes severe membrane fouling in membrane filtration [59, 60].

1.4 Ozonation of NOM

In ozonation, NOM affects ozone stability because it is involved in both direct reaction with the ozone molecule and the indirect oxidation involving the ·OH [29]. The oxidation of NOM in both pathways produces biodegradable by-products, such as organic acids, aldehydes (formaldehyde, acetaldehyde, glyoxal and methyl-glyoxal) and ketoacids [56, 61]. These by-products, however, react slowly with ·OH.

NOM can directly consume ozone as well as react as the initiator, promoter and inhibitor simultaneously [26]. The quantification of rate constants of NOM in these reaction modes remains a challenge because these reactions collectively contribute to the ozone decomposition and ·OH formation/consumption, which cannot be isolated for study [26, 28, 29, 62, 63]. Westerhoff *et al.* [28] attempted a modeling approach by assigning the initiation, promotion and inhibition rate constants to NOM to fit the pseudo first-order kinetics of ozone decomposition. These assigned rate constants, however, were arbitrary and limited in value due to the lack of system calibration with an ·OH probe compound [29].

1.5 Ozonation of pharmaceutical compounds

The presence of pharmaceutical compounds in aquatic environment is an emerging problem that will considerably impact aquatic organisms and eventually human [64]. They have been frequently found in surface water and are largely contributed by wastewater effluents [65-67]. One of the most frequently detected pharmaceuticals in wastewater and surface waters is ibuprofen with concentrations ranging from ng/L to μg/L [67-73].

The removal of pharmaceuticals has been studied in different stages of drinking water treatment [74]. It was found that microbial biodegradation and activated carbon adsorption do not effectively eliminate pharmaceuticals due to the presence of NOM which competes in the removal processes [75]. Ozonation, on the other hand, has shown great potential to remove pharmaceuticals when incorporated in drinking water treatment processes [74, 76-79].

The degradation of pharmaceutical compounds during water ozonation can be modeled by considering the simultaneous removal by ozone and ·OH if the R_{ct} value (Section 1.2) in the system is determined [27]. The degradation of a pharmaceutical compound, denoted as P, is given by:

$$-\frac{d[P]}{dt} = k_{\cdot OH/P}[\cdot OH][P] + k_{O_3}[O_3][P] \tag{1.10}$$

where $k_{\cdot OH/P}$ and k_{O_3} represent the second order reaction rate constants of pharmaceutical compounds with ·OH and ozone, respectively.

Integrating Equation (1.10) gives the following:

$$\ln\left(\frac{[P]_t}{[P]_0}\right) = -(k_{\cdot OH/P}\int[\cdot OH]dt + k_{O_3}\int[O_3]dt) \tag{1.11}$$

Combining Equation (1.8) into Equation (1.11) yields

$$\ln\left(\frac{[P]_t}{[P]_0}\right) = -(k_{\cdot OH/P} R_{ct} + k_{O_3}) \int [O_3] dt \quad (1.12)$$

The ozone exposure can be determined using the following equation:

$$\int [O_3] dt = \frac{[O_3]_0}{k_{obs}} \left(1 - e^{-k_{obs} t}\right) \quad (1.13)$$

where k_{obs} can be experimentally determined and theoretically calculated using Equation (1.1) if the system is well-characterized.

The use of R_{ct} avoided difficulties arising from the calibration of the kinetic model in complex natural systems.

A study conducted by Huber *et al.* [77] showed that the second order rate constants of ozone (k_{O_3}) and ·OH ($k_{\cdot OH}$) for selected pharmaceuticals range from < 0.8 $M^{-1}s^{-1}$ to 2.5×10^6 $M^{-1}s^{-1}$ and 3.3×10^9 $M^{-1}s^{-1}$ to 9.8×10^9 $M^{-1}s^{-1}$, respectively. The greater variation of k_{O_3} is caused by that ozone reacts easily with pharmaceutical compounds containing phenolic and aromatic moieties [78]. Westerhoff *et al.* [78] studied the oxidation of pharmaceutical compounds with chlorine and ozone. They found that ozone and chlorine both react easily with pharmaceutical compounds containing aromatic ring structures but react poorly with those containing aliphatic moieties with polar functional groups. Some compounds showed greater degradation in ozonation due to the oxidation by ·OH produced in ozone decomposition. However, high concentrations of NOM were found to inhibit the removal of ·OH-reactive compounds by ozonation [79], and the detailed role of NOM was not evaluated.

1.6 Objectives

The objectives of this study were to develop a new method to quantify the initiation, promotion and inhibition rate constants of NOM and to quantitatively describe its influences on the removal of pharmaceutical compound during water ozonation. It was hypothesized that the integration of the ·OH transient steady-state model, R_{ct} concept and pseudo-first-order ozone decomposition model would allow the determination of these rate constants of NOM. Following tasks were conducted:

a. A new method that can be used to experimentally quantify the rate constants of the initiator, promoter and inhibitor that are simultaneously present in water ozonation was developed and validated. Representative model compounds were used.
b. The feasibility of the new method to determine the NOM rate constants as the initiator, promoter and inhibitor in an ozonation system was demonstrated using three NOM isolates and a natural water.
c. The influences of NOM on the degradation of ibuprofen, were determined and modeled.

1.7 Significance of the study

The degradation of organic contaminants including pharmaceutical compounds by water ozonation relies strongly on the oxidative capability of ozone and ·OH. The contribution of ubiquitous NOM on the ozone decomposition and the formation/consumption of ·OH plays an important role in the removal of target

contaminants but its effects are not clearly understood. The results of this study provide the fundamental understanding of the kinetic behaviors of NOM in ozonation which has not been reported before. In addition, the knowledge of NOM behaviors in ozonation might be used to optimize the design and operation of the ozonation process on the removal of organic pollutants.

1.8 Thesis Organization

This thesis contains six chapters. In Chapter 2, the experimental setup and analytical methods employed are described. The results and discussion are presented in Chapter 3, 4 and 5. Chapter 3 presents the development and validation of a new method that can be used to experimentally quantify the initiation, promotion and inhibition rate constants in water ozonation. The new method was verified using model compounds that are representative of initiator, promoter and inhibitor. Chapter 4 illustrates the applicability of this new model in the determination of the initiation, promotion and inhibition rate constants of NOM using three NOM isolates, including Suwannee River humic and fulvic acids and a commercial humic acid (Sigma-Aldrich), and a natural water. The influences of NOM on the removal of ibuprofen by water ozonation using the rate constants determined in Chapter 4 is explored and modeled in Chapter 5. Finally, Chapter 6 summarizes the findings of this research and provides some recommendations for further studies.

CHAPTER 2

MATERIALS AND METHODS

2.1 Reagents and chemicals

Reagent grade and analytical grade chemicals were used in this study. All chemicals were used as received without further purification. Potassium indigo trisulfonate, sodium thiosulfate, pCBA, formic acid, *tert*-butanol and ibuprofen were supplied by Sigma-Aldrich. Potassium iodide, sodium acetate, sodium hydrogen phosphate (Na_2HPO_4), sodium dihydrogen phosphate (NaH_2PO_4), methanol, acetonitrile, sodium hydroxide (NaOH), phosphoric acid and hydrochloric acid (HCl) were purchased from Merck. All stock and experimental solutions used in this study were prepared by ultrapure water, generated from a Milli-Q Direct 8 Ultrapure Water Systems (Millipore) consisting of activated carbon, reverse osmosis, ion exchange and a 0.22 μm membrane filter.

2.2 Stock Solutions

2.2.1 Ozone, indigo and phosphate buffer stock solutions

Aqueous ozone stock solution was freshly prepared before each experiment by bubbling ozone gas through ultrapure water using gas washing bottles cooled in an ice bath. Ozone gas was generated by the Anseros ozone generator (Model COM-AD-02) using pure oxygen as the feed gas. Residual ozone gas in the effluent of the gas washing bottle was quenched by concentrated potassium iodide solutions. All tubing used was made of Teflon PTFE/PFA in order to avoid contamination of the gas stream. The ozone concentration in the stock solution was determined using the UV

spectrometric method. Typically, after two hours of purging, the ozone concentration in the stock solution ranged from 50 to 60 mg/L.

Indigo stock solution (0.77 g/L) was prepared by dissolving 0.154 g of potassium indigo trisulfonate in 200 mL of ultrapure water that was pre-acidified to pH 2.0 by 0.2 mL of concentrated phosphoric acid. Indigo reagent II solution that is used for measuring ozone concentration greater than 0.3 mg/L was prepared by mixing 5.0 mL of indigo stock solution, 5.0 g of NaH_2PO_4 and 0.35 mL of phosphoric acid according to the procedure described in the Standard Methods [80].

1.0 M phosphate buffer was prepared by dissolving Na_2HPO_4 and NaH_2PO_4 in 100 mL of ultrapure water.

2.2.2 NOM stock solutions

Three NOM isolates, including Suwannee River humic and fulvic acids (SRHA and SRFA, respectively), and Sigma-Aldrich humic acid (SAHA) were used in this study. SRHA and SRFA were purchased from the International Humic Substances Society and SAHA was purchased from Sigma-Aldrich. SRHA and SAHA stock solutions were prepared following the procedures described in the literature [26], but HCl was used rather than perchloric acid for pH adjustment. 0.05 g of SRHA and 0.2 g of SAHA were dissolved in 100 mL ultrapure water that was pre-adjusted to pH 10.5 by 1.0 M NaOH. The solutions were stirred by a magnetic bar for two hours before they were filtered through a 0.45 μm nylon membrane filter (Whatman) to remove any remaining particulate fraction. The pH of the SRHA and SAHA filtrates were adjusted to pH 4.0 with 1.0 M HCl. The filtrates were later stored in the refrigerator and used in subsequent experiments. The SRFA stock

solution was prepared by dissolving 0.05 g of SRFA in 100 mL ultrapure water without pH adjustment. The carbon content and specific UV absorbance at 254 nm ($SUVA_{254}$) of SRHA, SRFA and SAHA were determined to be 0.46, 0.47 and 0.44 (mg C) per mg NOM and 8.7, 5.5, 7.3 L $(mg\ C)^{-1}\ m^{-1}$, respectively.

2.2.3 pCBA and ibuprofen stock solutions

The 0.32 mM pCBA stock solution was prepared by dissolving 5 mg of pCBA in 100 mL of ultrapure water. Since pCBA is unable to dissolve in ultrapure water at room temperature, the solution was boiled for 30 min during the preparation.

The 0.24 mM ibuprofen stock solution was prepared by dissolving 10 mg of ibuprofen in 200 mL of ultrapure water. Similar to pCBA, the ibuprofen solution was boiled for 45 min.

2.3 Natural water

Water collected from a local reservoir in Singapore was used in this study and was filtered with a 0.45 μm pore size nylon membrane (Whatman) and stored at 4 °C until use. The filtered water possessed the following characteristics: pH 7.4, dissolved organic carbon (DOC) = 2.3 (mg C)/L, alkalinity = 39 mg L^{-1} as $CaCO_3$, UV_{254} = 0.05 cm^{-1}, and $SUVA_{254}$ = 2.2 L $(mg\ C)^{-1} \cdot m^{-1}$.

2.4 Ozonation experiments

All ozonation experiments were conducted in batch mode using a 1 L glass bottle equipped with a 10 mL bottle-top dispenser [81]. The ultrapure water used to

prepare experimental solutions was pre-ozonated to minimize its ozone demand. Prior to each experiment, the pre-ozonated ultrapure water was first acidified to pH 3.5 by concentrated HCl followed by nitrogen gas purging for 30 min to remove dissolved inorganic carbon (HCO_3^- and CO_3^{2-}) that can serve as the inhibitor in the ozonation process [27]. The solution pH was adjusted to the desired value using 1.0 M NaOH and HCl under a gentle stream of nitrogen gas. 1.0 mM phosphate buffer was used to avoid fluctuations of pH during the course of the experiment.

pCBA (0.5 μM) was used as the ·OH probe compound. The low concentration of pCBA did not contribute significantly to the total scavenging capacity of ·OH in this study [27]. After adding the desired chemicals, ozone was added to the solution to initiate the reaction if not stated otherwise. Samples were collected using the bottle-top dispenser at designated time for a period of up to 30 min for the measurements of ozone, pCBA and ibuprofen. To stop further degradation of pCBA and ibuprofen, ozone was quenched with sodium thiosulfate (0.025 M). All experiments were conducted at 21±1 ℃.

2.4.1 Validation of the new R_{ct} expression and the new method for the determination of rate constants of initiator, promoter and inhibitor in water ozonation

The new R_{ct} expression and the new method for the determination of rate constants of initiator, promoter and inhibitor described in Chapter 3 were validated using simple model compounds. Hydroxide ion (k_{O_3} or k_1 = 70 M^{-1} s^{-1} [82]), methanol (k_{O_3} = 0.024 $M^{-1}s^{-1}$ [19]; $k_{\cdot OH}$ = 9.7×10^8 $M^{-1}s^{-1}$ [23]) or formic acid (k_{O_3} = 100 $M^{-1}s^{-1}$ [83]; $k_{\cdot OH}$ = 3.2×10^9 $M^{-1}s^{-1}$ [23]), and acetate (k_{O_3} = 3×10^{-5} [83]; $k_{\cdot OH}$ = 7.9×10^7 $M^{-1}s^{-1}$

[23]) or *tert*-butanol (k_{O_3} = 0.003 $M^{-1}s^{-1}$ [19]; $k_{\cdot OH}$ = 6.0×10^{8} $M^{-1}s^{-1}$ [23]) were used as the model initiator, promoter and inhibitor, respectively. The selected compounds were chosen based on their ozone and ·OH second-order reaction rate constants as well as the products that formed upon their reactions with ozone and ·OH [19, 26, 82, 83]. The experimental conditions employed for the validations are compiled in Table 2.1, in which Run 1 to Run 4 were used to validate the new R_{ct} expression and Run 5 was used to validate the new method. In all experiments, ozone stock solution was added to achieve the desired initial ozone concentration of 48 μM or 2.3 mg/L after the addition of model compounds and pH value adjustment to initiate the reaction. The pH values were consistent during the course of the experiments, with a maximum variation of 0.1 pH unit.

Table 2.1. Experimental conditions employed in model compounds system for the validation of the new method

Model Compound	Run 1 (Effect of initiator concentration on R_{ct})	Run 2 (Effect of promoter concentration on R_{ct})	Run 3 (Effect of promoter concentration on R_{ct})	Run 4 (Effect of inhibitor concentration on R_{ct})	Run 5 (Experimental quantification of the initiator, promoter and inhibitor rate constants)
OH^- (M)	1×10^{-7}-3.2×10^{-6} (pH 7.0-8.5)	1×10^{-6} (pH 8.0)	1×10^{-6} (pH 8.0)	1×10^{-6} (pH 8.0)	1×10^{-6} (pH 8.0)
Methanol (mM)	0.1	0-0.25	-	0.1	0.1
Formic Acid (mM)	-	-	0-0.075	-	-
tert-butanol (mM)	0.05	0.05	0.05	0.01-0.1	0.01-0.1
Acetate (mM)	-	-	-	-	0.1

2.4.2 Determination of the rate constants of NOM isolates and natural water NOM as the initiator, promoter and inhibitor

The applicability of the kinetic model on the quantification of NOM rate constants as the initiator, promoter and inhibitor was demonstrated using three different NOM isolates including SRHA, SRFA and SAHA and a natural water. The experiments were conducted at a fixed pH value (8.0) and NOM concentration (2.0 mg/L). The only variation was the external inhibitor (*tert*-butanol) concentration which ranged from 0.03 to 0.3 mM. For natural water experiments, the water was used without any alteration except for the addition of phosphate buffer (1.0 mM) and pCBA (0.5 μM). In order to satisfy the instantaneous ozone demand, an initial ozone concentration of 100 μM (4.8 mg/L) was employed. It was found that the variations of pH value in the end of experiments were within ±0.1 pH unit.

2.4.3 The influences of NOM on the degradation of ibuprofen by ozonation

In the experiments of ibuprofen degradation, an initial ibuprofen concentration of approximately 0.5 μM (100 μg/L) was used. This was higher than those found in the environments in order to allow a mechanistic study on the influence of NOM on its degradation. SRFA was selected as a NOM representative with the concentration ranging from 0 to 4.0 mg/L. The pH and carbonate alkalinity employed in this study were 7.0 and 2.0 mM, respectively. The removal of ibuprofen in this study was investigated under two conditions: 1. ibuprofen was removed in both the first (< 20 s) and second (> 20 s) R_{ct} stages and 2. ibuprofen was removed only in the second R_{ct} stage. In condition 1, ibuprofen was added at the beginning when ozonation was initiated. For condition 2, ibuprofen was added 70 s after the ozonation was initiated.

The pH values measured at the end of each experiment was found to be within ±0.1 pH unit.

2.5 Analytical methods

2.5.1 Ozone concentration measurement

Aqueous ozone concentration was measured by a UV spectrophotometer (Shimadzu UV-1800). The dissolved ozone stock solutions concentrations were determined directly by measuring their UV absorbance at 258 nm (ε = 3100 $M^{-1}cm^{-1}$). The ozone stock solution was diluted once prior to its measurement to minimize the fluctuation of the UV absorbance. The ozone concentration is determined by the Beer's Law according to the following equation:

$$[O_3] = \frac{2(MW)(Abs)(1000)}{(b)(\varepsilon)} \tag{2.1}$$

where, $[O_3]$ represents ozone concentration (mg/L), MW represents molecular weight of ozone (g/mol), Abs represents absorbance at 258 nm, b represents cell length (cm) and ε represents extinction coefficient, L $mol^{-1}cm^{-1}$.

Dissolved ozone concentration in reaction solutions was determined using the indigo method [80, 84]. Typically, 1 mL of indigo reagent II solution was added into several 20 mL glass vials. One glass vial was filled with ultrapure water to 10 mL; while the others contained a mixture of the sample (ranging from 2 to 9 mL) and ultrapure water making the total volume of 10 mL. This series of dilution was to ensure that ozone decolorizes approximately 20 to 90% of the indigo reagent II

solution without completely bleaching the indigo solution. The absorbance at 600 nm of the blank and diluted samples was then measured. The ozone concentration was determined using Equation (2.2):

$$[O_3] = \frac{(\Delta Abs)(V_T)}{(f)(b)(V_S)} \tag{2.2}$$

where, ΔAbs represents difference in absorbance at 600nm between sample and blank, V_T represents the total volume of sample plus indigo (mL), V_S represents sample volume (mL) and f is 0.42 L (mg O_3)$^{-1}$ cm^{-1} which is obtained based on a sensitivity factor of 20 000 cm^{-1} for the absorbance of 600 nm per mole of added ozone per liter [84].

2.5.2 pCBA and ibuprofen measurement

A high performance liquid chromatography (HPLC) system (HPLC 1200 series, Agilent Technologies) equipped with an autosampler and a quaternary pump coupled with variable wavelength detector (VWD) was used for the measurement of pCBA concentration. Analysis was performed using 150 x 2.1 mm Zorbax SB-C18 column (Agilent Technologies). pCBA was eluted using an isocratic mobile phase of 55% methanol: 45% 10 mM phosphoric acid buffer at 0.2 mL/min, UV-detection at 234 nm and temperature was maintained at 25ºC [27]. The minimum detection limit determined from 8 replicates of 3.2×10^{-2} μM was 3.8×10^{-3} μM.

Same equipment and column were used for ibuprofen measurement. However, instead of an isocratic elution, ibuprofen was eluted using a binary gradient mobile phase consisting of mobile phase A (acetonitrile: phosphoric acid: water = 34 %: 0.05

%: 65.95 %) and B (100% acetonitrile) with a flow rate of 0.2 mL/min and detected at 214 nm at 30 ^{o}C. The minimum detection limit determined from 8 replicates of 2.4×10^{-2} μM was 1.6×10^{-2} μM.

2.5.3 Dissolved organic carbon measurement

The Shimadzu TOC-VCSH analyzer was used for DOC measurements. The minimum detection limit determined from 8 replicates of 0.5 (mg C)/L was 0.1 (mg C)/L.

2.5.4 pH measurement

The pH value was measured using a Horiba pH meter equipped with a Accumet pH electrode (Fisher Scientific) calibrated with pH 4, 7 and 10 standard buffers (Fisher Scientific).

CHAPTER 3

METHOD DEVELOPMENT FOR THE DETERMINATION OF RATE CONSTANTS OF INITIATOR, PROMOTER AND INHIBITOR PRESENT SIMULTANEOUSLY IN WATER OZONATION

NOM can simultaneously act as the initiator, promoter and inhibitor in water ozonation. Although extensive studies have been conducted on the ozone decomposition in the presence of NOM, quantitative evaluation of NOM rate constants in terms of these reactions are still lacking. A new approach simultaneously considering the kinetic behaviours of initiator, promoter and inhibitor in water ozonation is required to solve this problem. In this chapter, a new method integrating the ·OH transient steady-state, R_{ct} concept, and pseudo-first-order ozone decomposition model was developed to quantitatively determine the rate constants of initiator, promoter and inhibitor. The theoretical background is presented and the method is validated using simple model compounds representative of the initiator, promoter and inhibitor.

3.1 Missing links between existing models and method development

The new method that can be used to quantify the rate constants of initiator, promoter and inhibitor simultaneously present in water ozonation is based on a model formulated by integrating the ·OH transient steady-state (Equation (1.2)), R_{ct} concept (Equation (1.8)) and pseudo first-order ozone decomposition model (Equation (1.1)), which were studied separately and their links have never been explored. To establish the relationships among the three models, Equation (1.2) is first substituted into

Equation (1.8), leading to the following new R_{ct} expression if the solution pH, initiator concentration and inhibitor concentration remain constant during the course of ozonation:

$$R_{ct} = \frac{\int[\cdot OH]dt}{\int[O_3]dt} = \frac{\int\left(\frac{2k_1[OH^-]+\sum k_{I,i}[M_{I,i}]}{\sum k_{S,i}[M_{S,i}]}[O_3]\right)dt}{\int[O_3]dt} = \frac{2k_1[OH^-]+\sum k_{I,i}[M_{I,i}]}{\sum k_{S,i}[M_{S,i}]} \quad (3.1)$$

Equation (3.1) suggests that the R_{ct} value is not only the ratio of ·OH exposure to ozone exposure but also the ratio of the total initiation capacity ($2k_1[OH^-] + \Sigma k_{I,i}[M_{I,i}]$) to the total inhibition capacity ($\Sigma k_{s,i}[M_{s,i}]$) in an ozonation system. It also suggests that the presence of promoter does not affect the R_{ct} value.

Promoter can accelerate ozone decomposition since additional ozone is required to propagate the ·OH chain reactions (see Figure 1.1). Substitution of Equation (3.1) into Equation (1.1) yields the following equation:

$$-\frac{d[O_3]}{dt}\frac{1}{[O_3]} = k_{obs} = 3k_1[OH^-] + \sum(k_{D,i}[M_{D,i}]) + \sum(k_{I,i}[M_{I,i}]) + \sum(k_{P,i}[M_{P,i}])R_{ct} \quad (3.2)$$

Equation (3.2) suggests that k_{obs} is linearly correlated to the R_{ct} value.

The reciprocal of Equation (3.1) gives the following equation if an external inhibitor (S) possessing a second order rate constant k_{ss} with ·OH is added in the system:

$$\frac{1}{R_{ct}} = \frac{k_{SS}[S]+\sum k_{S,i}[M_{S,i}]}{2k_1[OH^-]+\sum k_{I,i}[M_{I,i}]} \quad (3.3)$$

With the addition of various concentrations of S, a plot of $1/R_{ct}$ vs. $k_{SS}[S]$ which would yield a straight line can be established, in which the initiation and inhibition capacities of the system can be determined from the slope $\left(\frac{1}{(2k_1[OH^-]+\sum k_{I,i}[M_{I,i}]}\right)$ and intercept $\left(\frac{\sum k_{S,i}[M_{S,i}]}{(2k_1[OH^-]+\sum k_{I,i}[M_{I,i}])}\right)$, respectively. If the concentrations of initiator and inhibitor are known, their respective rate constants can be calculated. The linear correlation between k_{obs} and R_{ct} shown in Equation (3.2) suggests that the promotion capacity can be determined from the slope ($\sum k_{P,i}[M_{P,i}]$) of the plot of k_{obs} vs. R_{ct}. Similar, if the concentration of promoter is known, its rate constant can be computed. The two plots of $1/R_{ct}$ vs. $k_{SS}[S]$ and k_{obs} vs. R_{ct} are depicted in Figure 3.1.

In summary, the new method requires the addition of various concentrations of an external inhibitor to the system and the values of k_{obs} and R_{ct} for each addition are measured. The two plots shown in Figure 3.1 are constructed. The rate constants of initiator, promoter and inhibitor can then be determined from the slope and intercept of the plots.

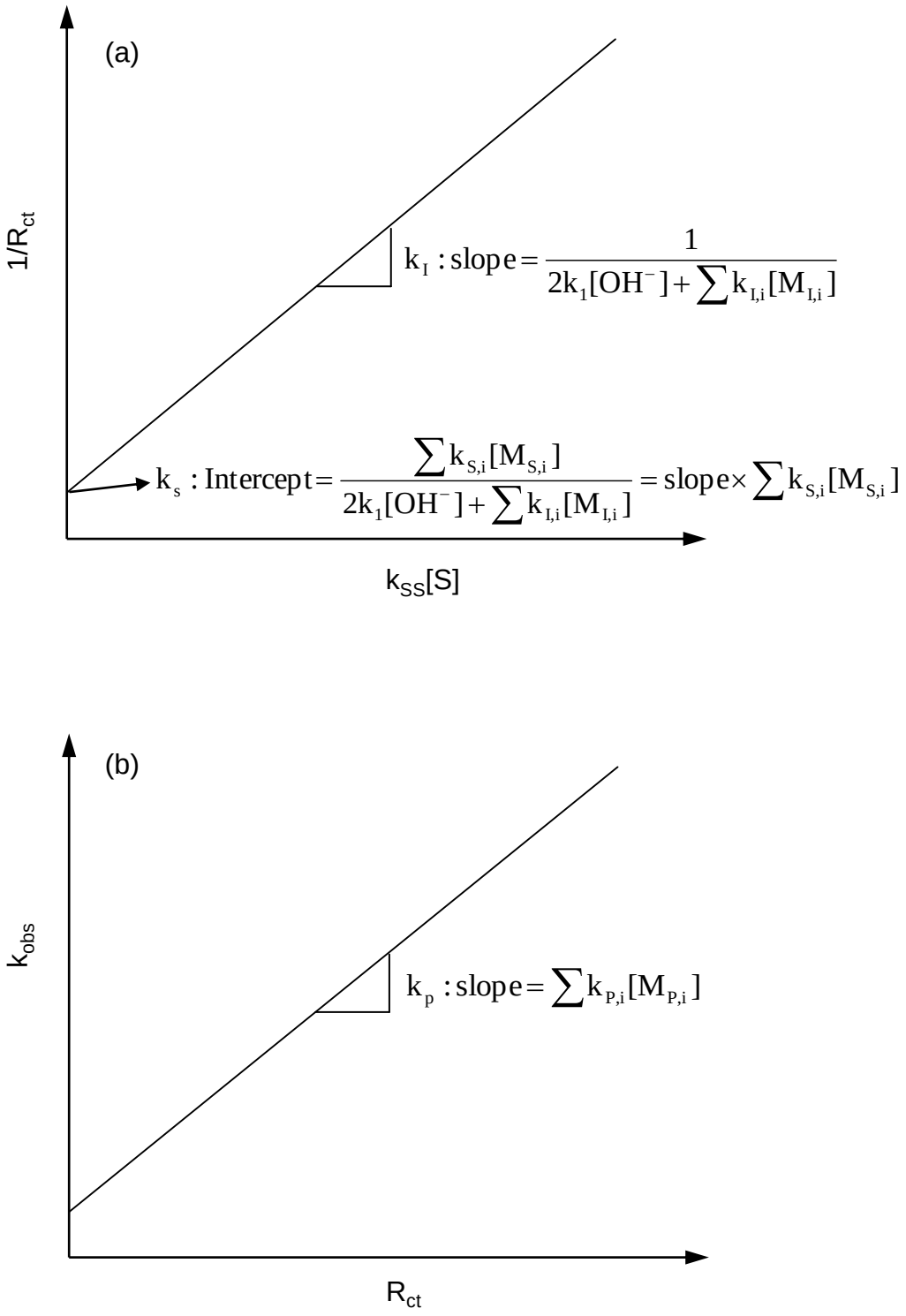

Figure 3.1 The theoretical relationship of (a) $1/R_{ct}$ plotted against ($k_{SS}[S]$) and (b) k_{obs} plotted against R_{ct}.

3.2 Validation of the new R_{ct} expression

The developed mathematical expression shown in Equations (3.1) needs to be verified prior to the validation of the proposed method to quantify the initiation, promotion and inhibition rate constants in water ozonation. A simple system consisting of one initiator (OH^-), one promoter (methanol or formic acid) and one inhibitor (*tert*-butanol) was employed. The respective formulations under this condition can be simplified as

$$R_{ct} = \frac{2k_1[OH^-]}{k_{SS}[S]} \tag{3.4}$$

where k_{SS} represents the second-order rate constant between OH and *tert*-butanol (S).

Two promoters (methanol and formic acid) at various concentrations were tested separately to first verify that the presence of promoter does not affect the R_{ct} value. Figure 3.2 shows the plots of R_{ct} using methanol (0-0.25 mM) or formic acid (0-0.075 mM) as the model promoters and Figure 3.3 shows the plot of R_{ct} value vs. promoter type and concentration. It should be noted that although formic acid can also act as an initiator [26], the concentration used in this study was too low for its initiation reaction to be significant compared to its promotion reaction. The R_{ct} values determined in the presence of these two different promoters were very consistent, ranging from 1.0×10^{-8} to 1.2×10^{-8} with an average of 1.1×10^{-8} and a standard deviation of 0.1×10^{-8}. Although the presence of promoter significantly accelerated the decomposition of ozone and slowed down the decay of pCBA (Figure 3.4 and 3.5),

these values were very close to those determined in the absence of promoter, i.e. 0.9×10^{-8} to 1.1×10^{-8} (average = 1.0×10^{-8}, standard deviation = 0.1×10^{-8}).

The ozone exposure and ·OH exposure determined from the experiments are shown in Figure 3.6. Both exposures decreased as the concentration of promoter increased while their ratio remained relatively constant. The decrease in the ozone exposure was due to the accelerated decomposition of ozone in the chain reactions propagated by the promoter. The decrease in the ·OH exposure was due to the lower transient steady-state ·OH concentration resulting from the accelerated ozone decomposition (Equation (1.2)).

Theoretically, the experimental conditions employed in these experiments (pH 8.0, *tert*-butanol = 0.05 mM) should yield a R_{ct} value of 4.7×10^{-9}, if k_1 = 70 $M^{-1}s^{-1}$ [82] and k_{ss} = 6.0×10^{8} $M^{-1}s^{-1}$ [23] were used. An accurate fit of the experimental data to this value was not achieved and the theoretical R_{ct} value was consistently about one half of those obtained in our experiments. It should be noted that k_1 = 70 $M^{-1}s^{-1}$ was determined in the presence of high carbonate and phosphate concentrations (10 mM and 50 mM, respectively), such that radical chain reactions were completely inhibited [82]. Larger values of k_1 have been reported in the literature when a lower inhibition capacity was employed [27, 85]. In fact, a k_1 value within a factor of 3, i.e. up to about 210 $M^{-1}s^{-1}$, has been considered as a good approximation [27]. Using the average R_{ct} value (1.1×10^{-8}) obtained in our experiments, a k_1 value of 160 $M^{-1}s^{-1}$ can be derived, which falls within an acceptable range considering the complexity of the system investigated.

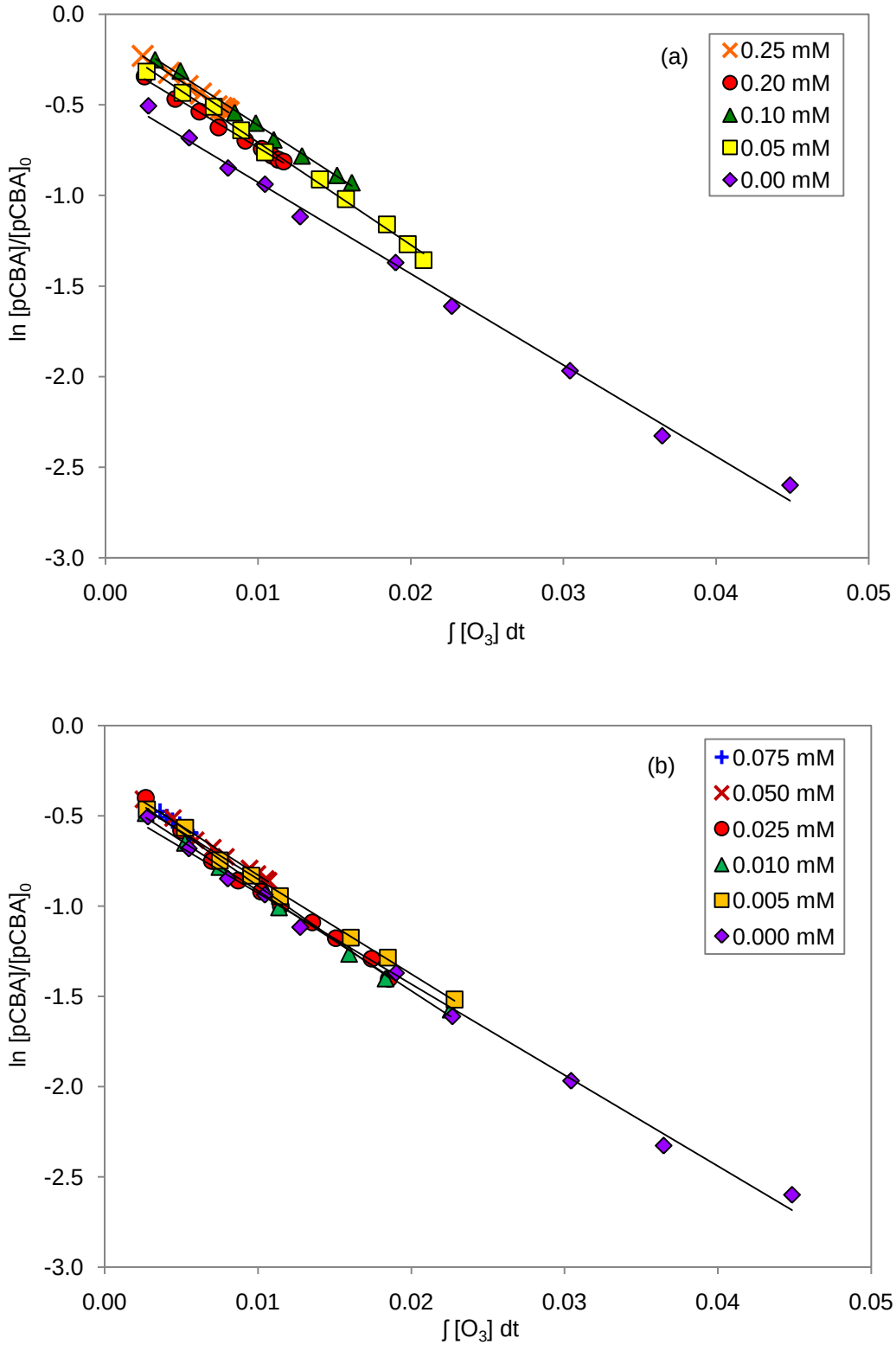

Figure 3.2 The R_{ct} plots for different concentrations of (a) methanol (0-0.25 mM) and (b) formic acid (0-0.075 mM). Experimental conditions: pH 8.0, initial ozone concentration = 48 µM, *tert*-butanol = 0.05 mM, pCBA = 0.5 µM and phosphate buffer = 1 mM.

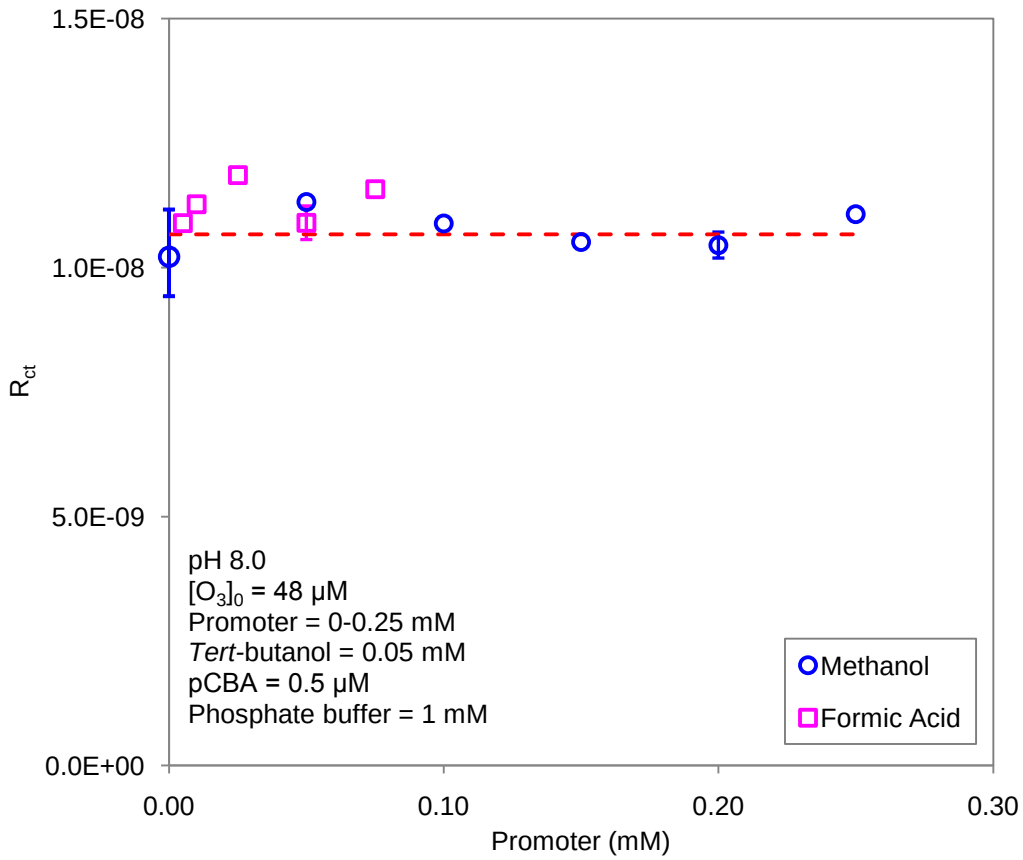

Figure 3.3 Effects of a promoter (methanol or formic acid) on the R_{ct} value. The dotted line represents the theoretical R_{ct} value computed using k_1 = 160 $M^{-1}s^{-1}$. The error bar represents the range of duplicates.

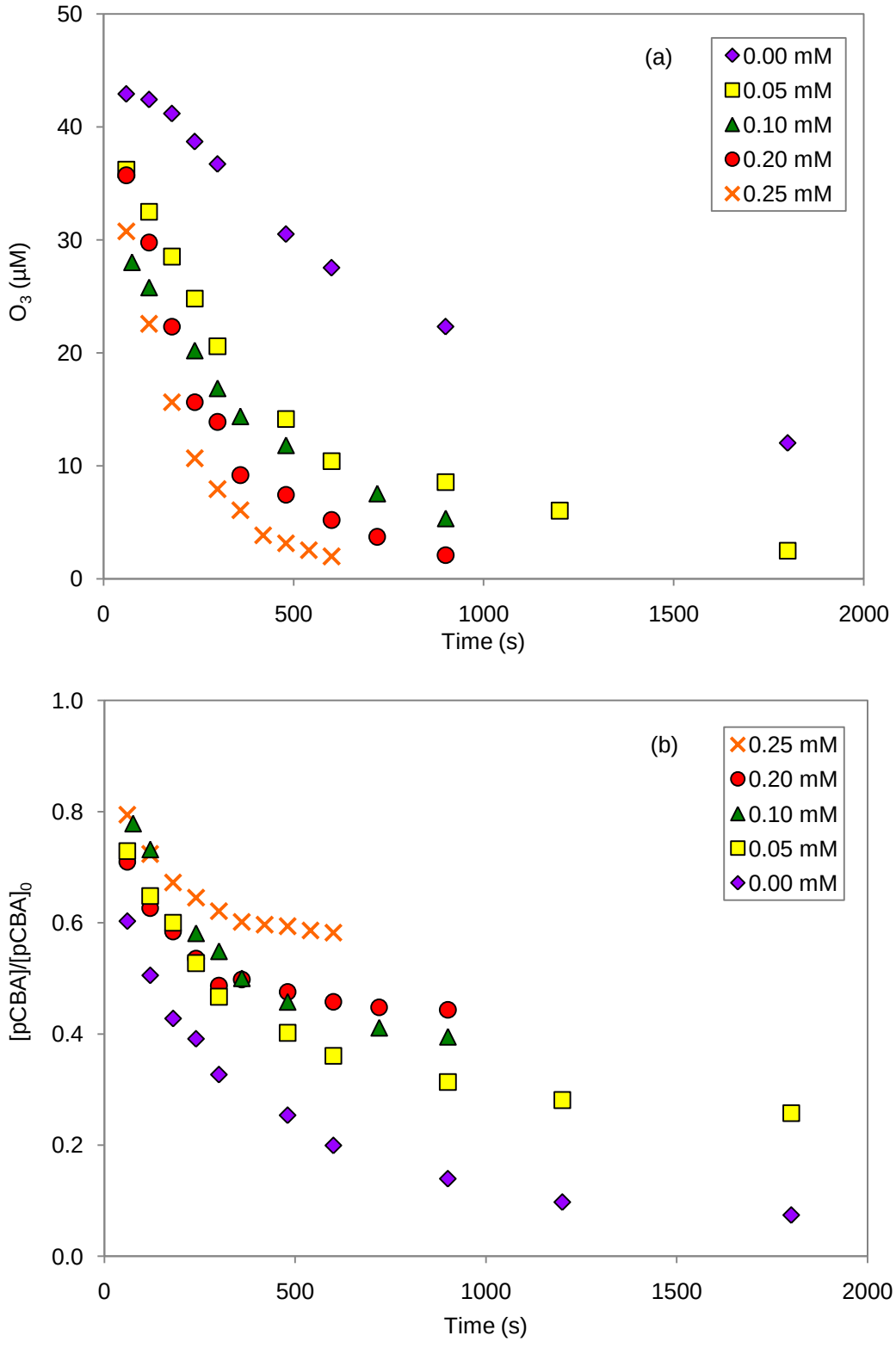

Figure 3.4 Effects of methanol concentration on (a) ozone decomposition and (b) pCBA decay versus time . Experimental conditions: pH 8.0, initial ozone concentration = 48 µM, *tert*-butanol = 0.05 mM, pCBA = 0.5 µM and phosphate buffer = 1 mM.

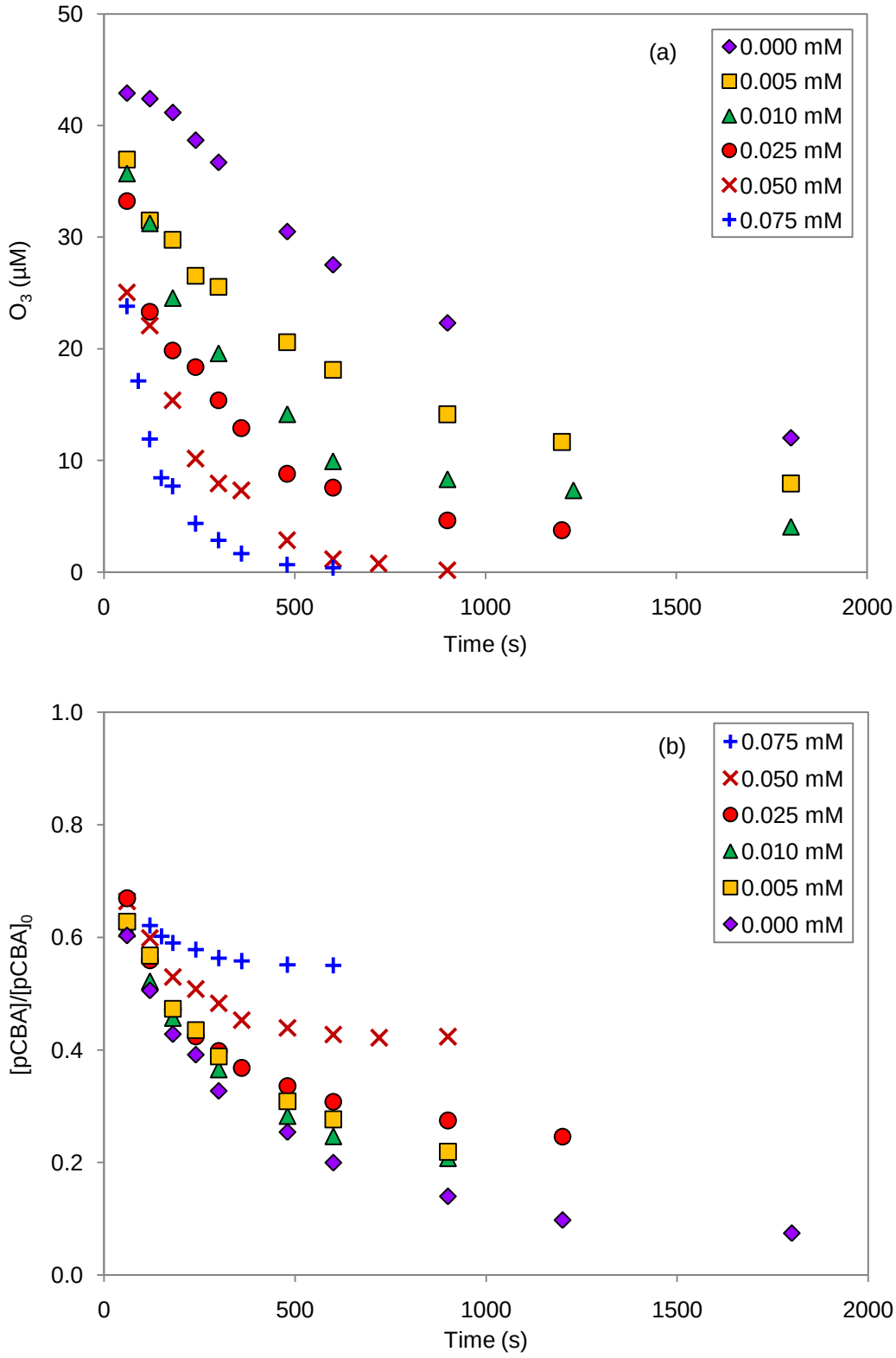

Figure 3.5 Effects of formic acid concentration on (a) ozone decomposition and (b) pCBA decay versus time . Experimental conditions: pH 8.0, initial ozone concentration = 48 µM, *tert*-butanol = 0.05 mM, pCBA = 0.5 µM and phosphate buffer = 1 mM.

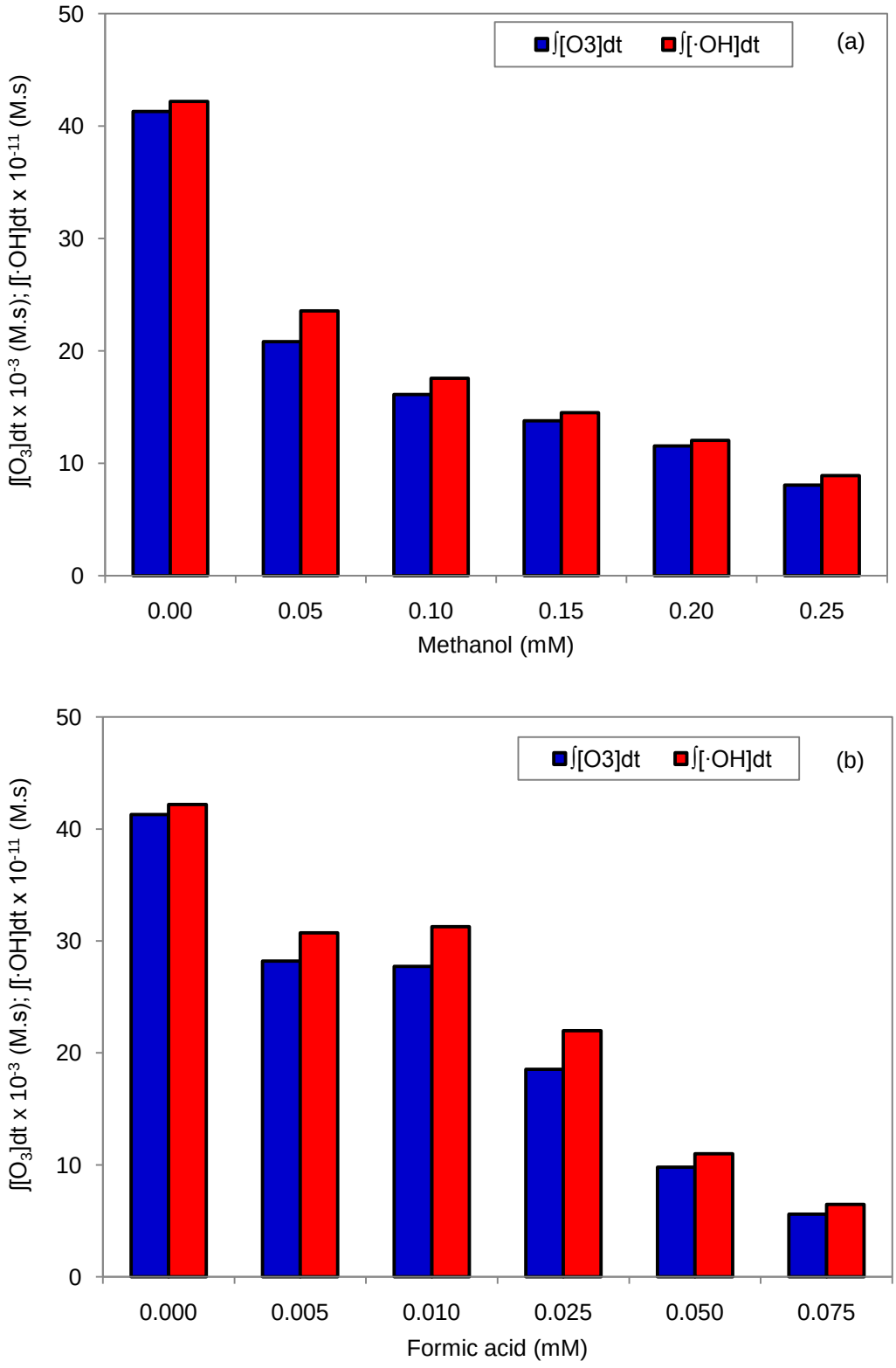

Figure 3.6 Ozone exposure ($\int[O_3]dt$) and ·OH exposure ($\int[\cdot OH]dt$) determined in the presence of different concentrations of (a) methanol and (b) formic acid. Experimental conditions: pH 8.0, initial ozone concentration = 48 µM, *tert*-butanol = 0.05 mM, pCBA = 0.5 µM and phosphate buffer =1 mM.

Figure 3.7 shows the R_{ct} values for pH 7.0-8.5 ($[OH^-] = 1.0\times10^{-7}$-$3.2\times10^{-6}$ M) in the presence of 0.1 mM of methanol and 0.05 mM of *tert*-butanol. The predicted R_{ct} value using $k_1 = 160\ M^{-1}s^{-1}$ is also shown. The corresponding decomposition of ozone and the decay of pCBA are presented in Figure 3.8. The rate of ozone decomposition increased with increasing pH due to the enhanced initiation reaction between OH^- and ozone that ultimately led to the formation of ·OH [26], which in turn, increased the R_{ct} value and the rate of pCBA decay. In general, the new R_{ct} model provides satisfactory simulations of the experimentally determined R_{ct} values.

Figure 3.9 shows the plot of R_{ct} value vs. the reciprocal of *tert*-butanol concentration (1/[S]) in the presence of 0.1 mM of methanol at pH 8.0. The predicted R_{ct} values using $k_1 = 160\ M^{-1}s^{-1}$ are also shown in the figure. A linear relationship was observed between the R_{ct} value and 1/[S], as illustrated by Equation (3.4), and the model predictions fitted well with experimental data. Both the rates of ozone decomposition and pCBA decay (Figure 3.10) decreased with the increasing *tert*-butanol concentration due to the reaction between *tert*-butanol and ·OH that terminated the chain reactions.

It should be noted that in the presence of oxygen, *tert*-butanol can react with ·OH to form peroxyl radical $(CH_3)_2C(OH)CH_2O_2\cdot$ and a bimolecular radical-radical reaction can lead to the formation of a tetraoxide that produces $\cdot O_2^-$ and H_2O_2 such that *tert*-butanol may not purely act as an inhibitor [86]. However, the formation of tetraoxide only occurs when the peroxyl radical concentration is sufficiently high [26, 86]. For the *tert*-butanol concentrations employed in this study (≤ 0.1 mM), such reaction appeared not to be important [26]. This is also evidenced by the slower rates of ozone decomposition and pCBA decay observed at higher *tert*-butanol

concentrations and the linear relationship observed between the R_{ct} value and 1/[S]. Thus, *tert*-butanol could serve as an ideal inhibitor in this study.

Overall, the influences of the initiator and inhibitor on the R_{ct} value agreed well with the new R_{ct} equation shown in Equation (3.1). It is also revealed that the presence of promoter does not affect the R_{ct} value but does accelerate ozone decomposition.

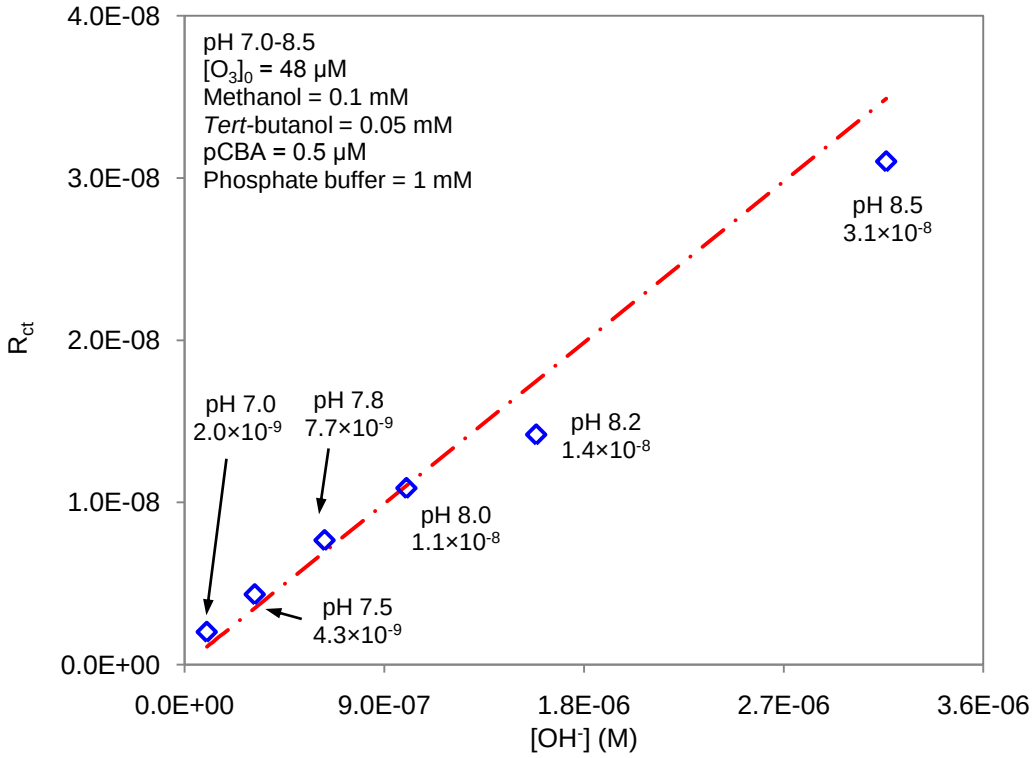

Figure 3.7 Effects of initiator (OH^-) on the R_{ct} value. The dotted line represents the theoretical R_{ct} value computed using $k_1 = 160\ M^{-1}s^{-1}$.

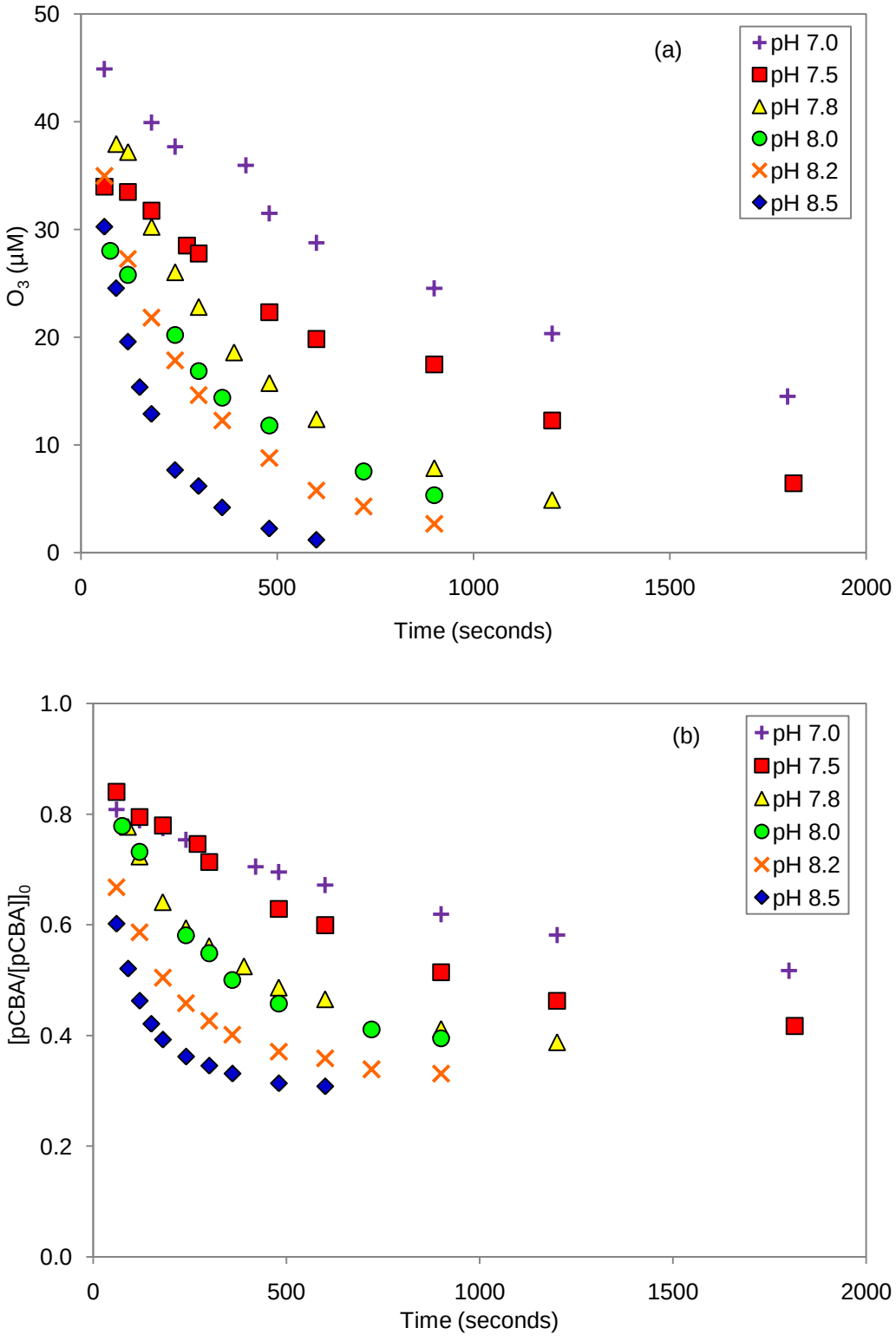

Figure 3.8 Effects of pH on the (a) decomposition of ozone and (b) pCBA decay versus time. Experimental conditions: Initial ozone concentration = 48 µM, methanol = 0.1 mM, *tert*-butanol = 0.05 mM, pCBA = 0.5 µM and phosphate buffer = 1 mM.

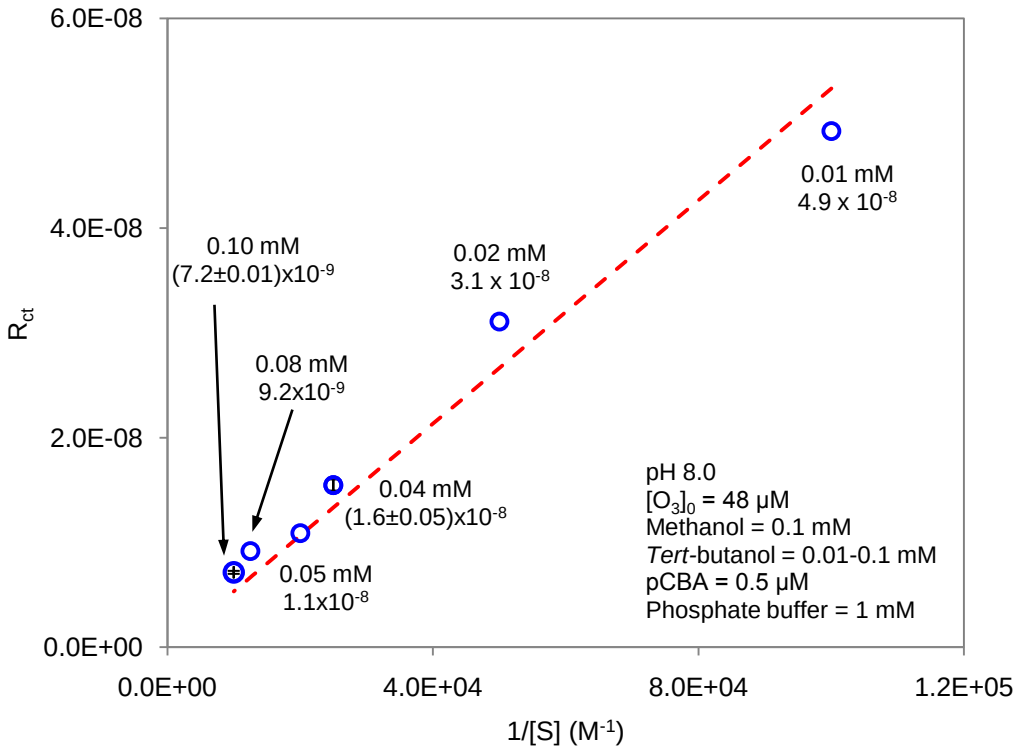

Figure 3.9 Effects of inhibitor (*tert*-butanol) on R_{ct} value. The dotted line represents the theoretical R_{ct} value computed using k_1 = 160 $M^{-1}s^{-1}$. The error bar represents the range of duplicates.

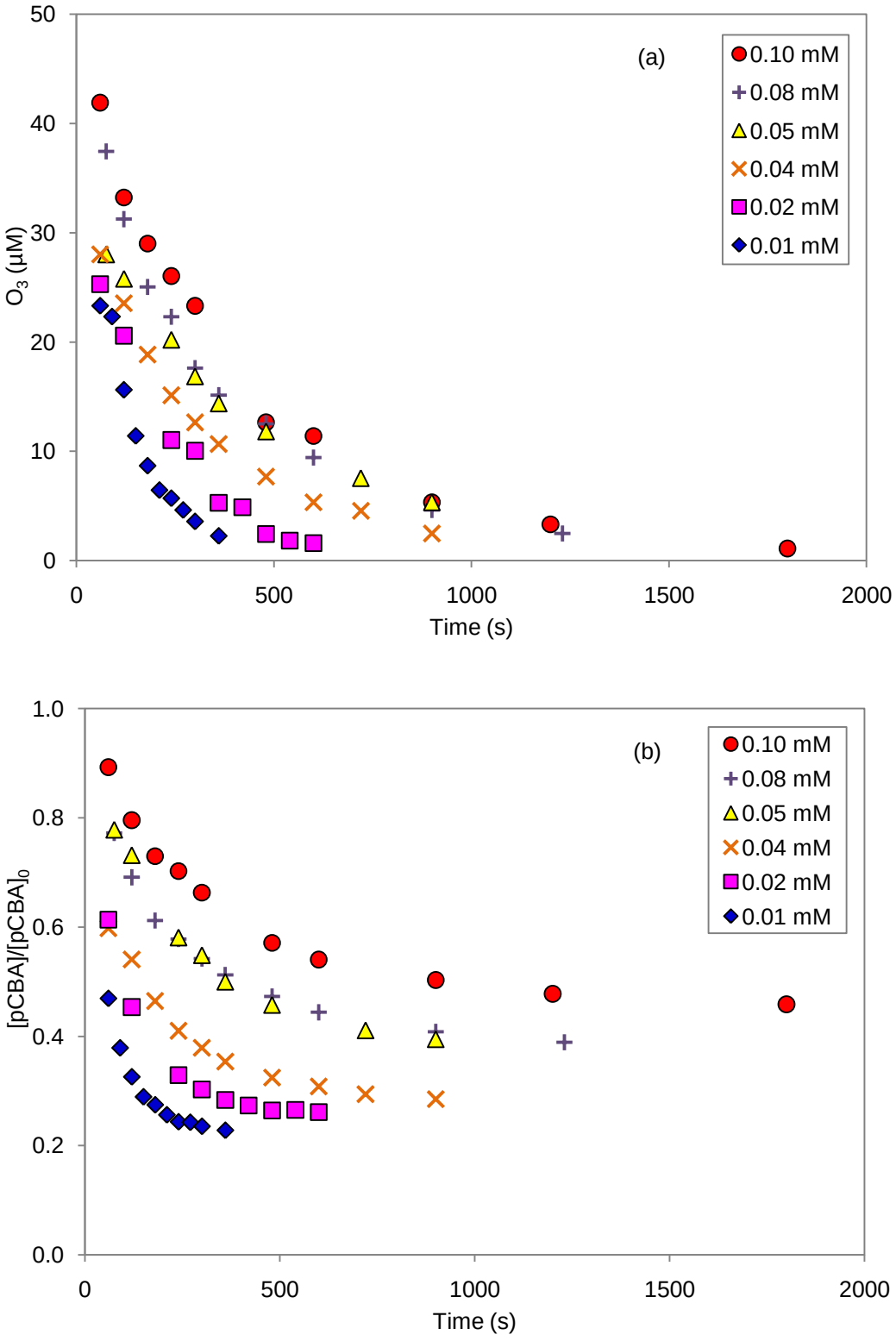

Figure 3.10 Effects of *tert*-butanol concentration on the (a) decomposition of ozone and (b) pCBA decay as a function of time. Experimental conditions: pH 8.0, initial ozone concentration = 48 µM, methanol = 0.1 mM, pCBA = 0.5 µM and phosphate buffer = 1 mM.

3.3. Validation of the proposed method for quantifying the initiation, promotion and inhibition rate constants in water ozonation

The validity of the proposed method for the determination of initiation, promotion and inhibition rate constants in water ozonation was demonstrated using a system containing model initiator (hydroxide ion), promoter (methanol) and inhibitor (acetate) with *tert*-butanol serving as the external inhibitor. Under such condition, the R_{ct} expression (Equation (3.1)) and the pseudo first-order ozone decomposition model (Equation (3.2)) can be rewritten as:

$$R_{ct} = \frac{2k_1[OH^-]}{k_{SS}[S] + k_S[M_S]} \tag{3.5}$$

$$-\frac{d[O_3]}{dt}\frac{1}{[O_3]} = k_{obs} = 3k_1[OH^-] + k_P[M_P]R_{ct} \tag{3.6}$$

Figure 3.11 shows the R_{ct} plots and ozone decomposition in the presence of 0.1 mM methanol and 0.1 mM of acetate at pH 8.0 with the addition of 0.01-0.10 mM *tert*-butanol. The R_{ct} and k_{obs} values determined from Figure 3.11 were used to construct the plots of $1/R_{ct}$ vs. $k_{SS}[S]$ and k_{obs} vs. R_{ct} as shown in Figure 3.12. The two plots followed the theoretical trends presented in Figure 3.1. The slope (3.1×10^3) and intercept (2.5×10^7) of $1/R_{ct}$ vs. $k_{SS}[S]$ (Figure 3.12(a)) can be used to determine k_I (or k_1 in this case) and k_S, respectively. The value of k_P can be determined from the slope (1.3×10^5) of the plot of k_{obs} vs. R_{ct} (Figure 3.12(b)). The determined k_1, k_S and k_P values along with their respective literature values were summarized in Table 3.1. The k_1 value computed using this approach, i.e. 161 $M^{-1}s^{-1}$, was in good agreement with the k_1 value obtained in Section 3.2. The k_S value calculated from the intercept of

Figure 3.12(a) was 8.2×10^{7} $M^{-1}s^{-1}$ which falls in the range of those obtained in previous studies, i.e. 7.9×10^{7} $M^{-1}s^{-1}$ to 8.5×10^{7} $M^{-1}s^{-1}$ [21, 23]. Finally, the k_P value was found to be 1.3×10^{9} $M^{-1}s^{-1}$ which only deviates slightly from one of the literature values (1.2×10^{9} $M^{-1}s^{-1}$ [87]) determined using the pulse radiolysis method.

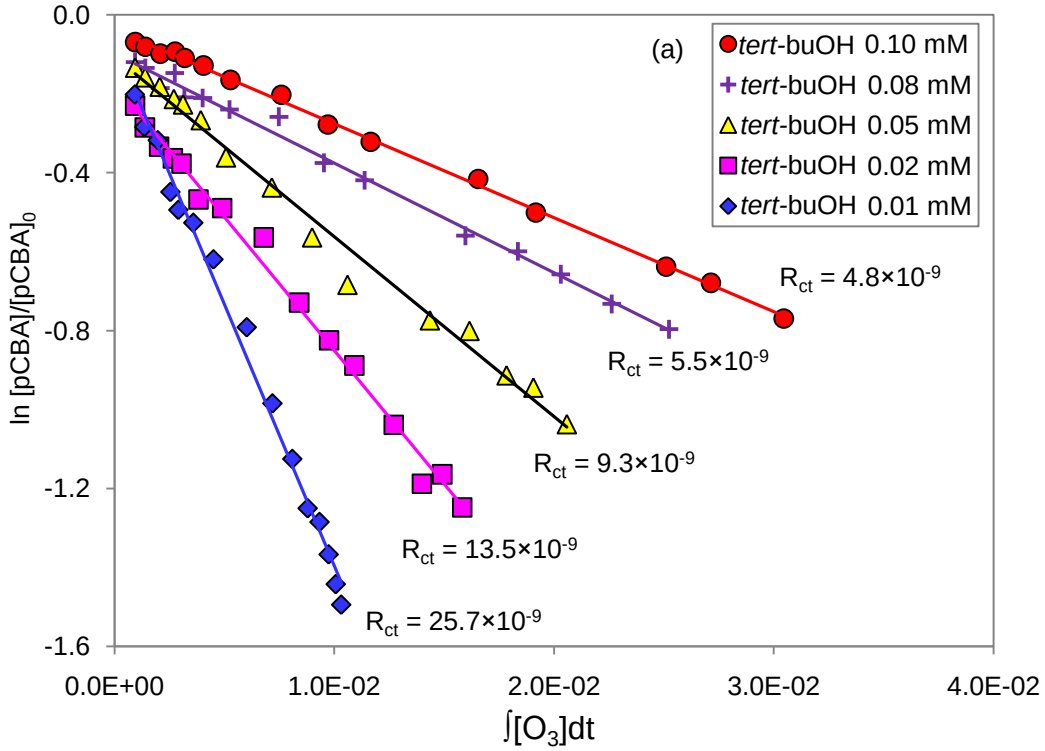

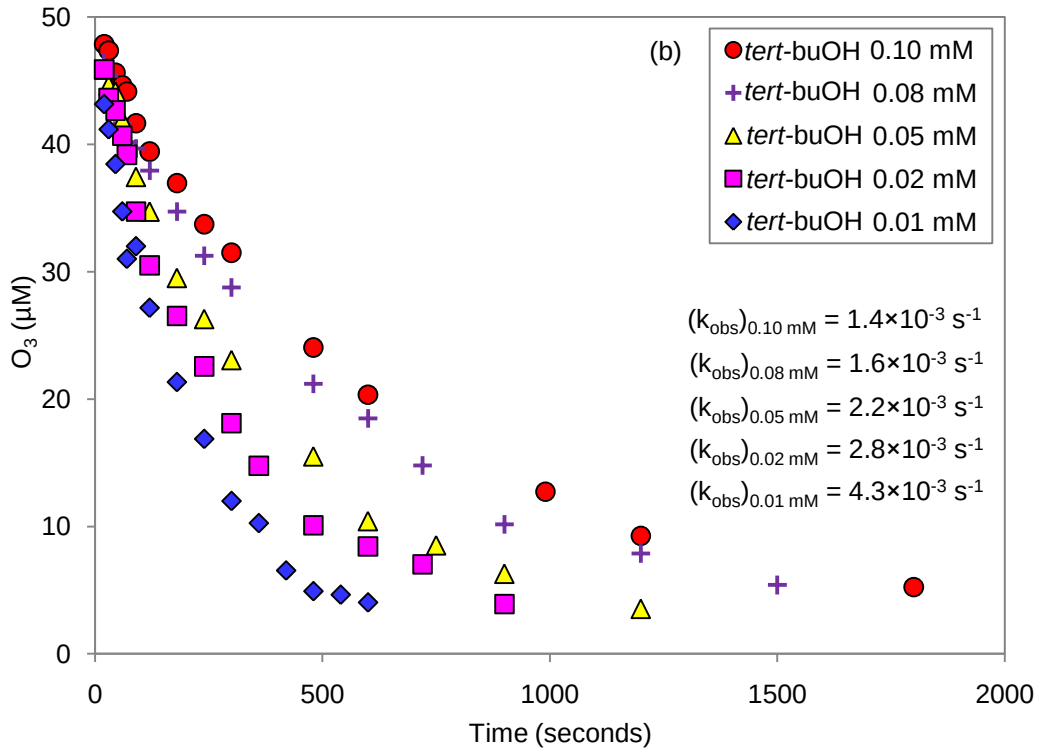

Figure 3.11 The (a) R_{ct} plot and (b) decomposition of ozone as a function of time in the presence of different *tert*-butanol concentrations ranging from 0.01 to 0.1 mM. Experimental conditions: pH 8.0, initial ozone concentration = 48 µM, methanol = 0.1 mM, acetate = 0.1 mM, pCBA = 0.5 µM and phosphate buffer = 1 mM.

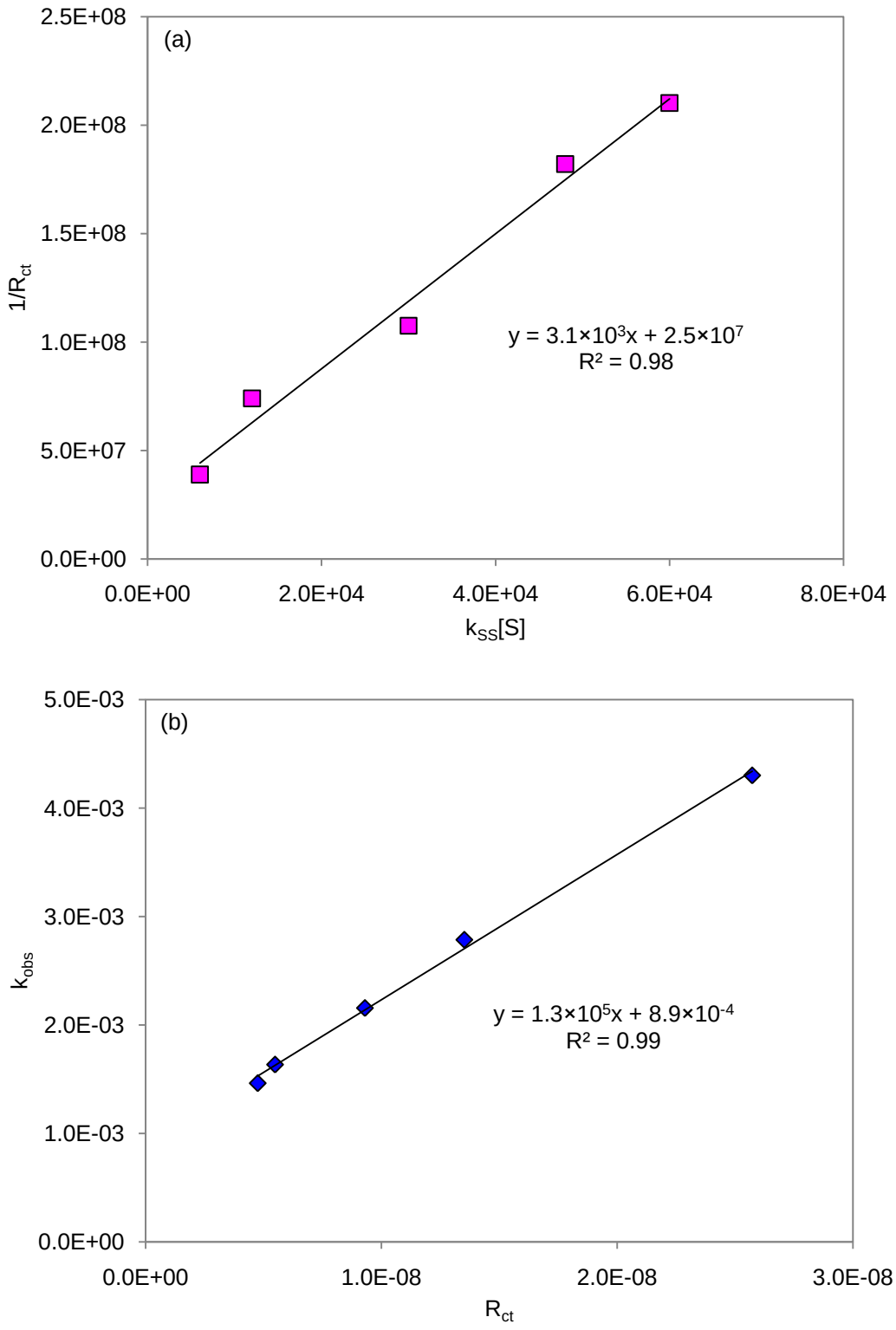

Figure 3.12 The graphical illustration of (a) $1/R_{ct}$ vs. $k_{SS}[S]$ and (b) k_{obs} vs. R_{ct} in the presence of model initiator (OH^- = 1.0×10^{-6} M; pH 8.0), promoter (methanol = 0.1 mM) and inhibitor (acetate = 0.1 mM) at various concentrations of *tert*-butanol (0.01-0.1 mM). Experimental conditions: Initial ozone concentration = 48 µM, pCBA = 0.5 µM and phosphate buffer = 1 mM.

Table 3.1 The compilation of the determined k_1, k_P and k_S values based on the newly developed method and their respective values obtained using pulse radiolysis method.

Model compounds	Reaction rate constants ($M^{-1}s^{-1}$)	Literature values ($M^{-1}s^{-1}$)	References
OH^- (k_1)	161	160	this study (Section 3.2)
Acetate (k_S)	8.2×10^7	7.9×10^7	[23]
		8.5×10^7	[21]
Methanol (k_P)	1.3×10^9	9.7×10^8	[23]
		1.2×10^9	[87]

3.4 Conclusions

The integration of ·OH transient steady-state, R_{ct} concept and pseudo first-order ozone decomposition model allows the experimental quantification of the rate constants of initiator, promoter and inhibitor that are simultaneously present in water ozonation. It is found that the R_{ct} value is not only the ratio of ·OH exposure to ozone exposure but also the ratio of the initiation capacity to the inhibition capacity of the ozonation system. In addition, the R_{ct} value is linearly correlated to the pseudo-first-order ozone decomposition rate constant.

With the addition of different concentrations of an external inhibitor S, the rate constants of initiator and inhibitor can be determined from the slope and intercept of the plot of $1/R_{ct}$ vs. $k_{SS}[S]$, respectively. The rate constant of promoter can be determined from the slope of the plot of k_{obs} vs. R_{ct}. This new approach is successfully verified using representative model compounds, which paves a way to quantitatively determine the initiation, promotion and inhibition rate constants of NOM in water ozonation, which will be discussed in Chapter 4.

CHAPTER 4

QUANTIFICATION OF THE RATE CONSTANTS OF NOM AS THE INITIATIOR, PROMOTER AND INHIBITIOR IN WATER OZONATION

The application of the method described in Chapter 3 for the determination of the rate constants of NOM as the initiator, promoter and inhibitor is demonstrated in this chapter. Three NOM isolates including Suwannee River humic acid (SRHA), Suwannee River fulvic acid (SRFA) and Sigma-Aldrich humic acid (SAHA) and NOM in a natural water collected from a reservoir in Singapore were used.

4.1 Application of the proposed method to the NOM system

To apply the method developed in Chapter 3 to a NOM system, the new R_{ct} expression in Equation (3.1) requires some modifications. At a fixed pH value, the addition of an external inhibitor (S, such as *tert*-butanol) to the system would transform Equation (3.1) into Equation (4.1) if dissolved organic carbon (DOC, mg C/L) is used to represent NOM and its initiation, promotion and inhibition reactions are simultaneously considered:

$$R_{ct} = \frac{2k_1[OH^-] + k_I[DOC]}{k_{SS}[S] + k_S[DOC]} \quad (4.1)$$

where k_I and k_S (unit: L(mg C)$^{-1}$s^{-1}) represent the initiation and inhibition rate constants of NOM, respectively.

The reciprocal of Equation (4.1) gives the following equation:

$$\frac{1}{R_{ct}} = \frac{k_{SS}[S] + k_S[DOC]}{2k_1[OH^-] + k_I[DOC]} \tag{4.2}$$

The plot of $1/R_{ct}$ vs. $k_{ss}[S]$ would yield a straight line with a slope of $\frac{1}{(2k_1[OH^-] + k_I[DOC])}$ and an intercept of $\frac{k_S[DOC]}{(2k_1[OH^-] + k_I[DOC])}$ as shown in Figure 4.1(a). The values of k_I and k_S of NOM, therefore, can be determined from the slope and intercept, respectively, with the known pH value and k_1.

For the same system, Equation (3.2) can be re-written as Equation (4.3):

$$-\frac{d[O_3]}{dt}\frac{1}{[O_3]} = k_{obs} = 3k_1[OH^-] + k_D[DOC] + k_I[DOC] + k_P[DOC]R_{ct} \tag{4.3}$$

where k_D and k_P (unit: $L(mg\ C)^{-1}s^{-1}$) represent the direct reaction and promotion rate constants of NOM, respectively.

The plot of k_{obs} vs. R_{ct} would yield a straight line with a slope of $k_p[DOC]$ and an intercept of $3k_1[OH^-]+k_D[DOC]+k_I[DOC]$ as shown in Figure 4.1(b). Thus, k_P can be determined from the slope of the plot. Additionally, k_D of NOM can be determined from the intercept.

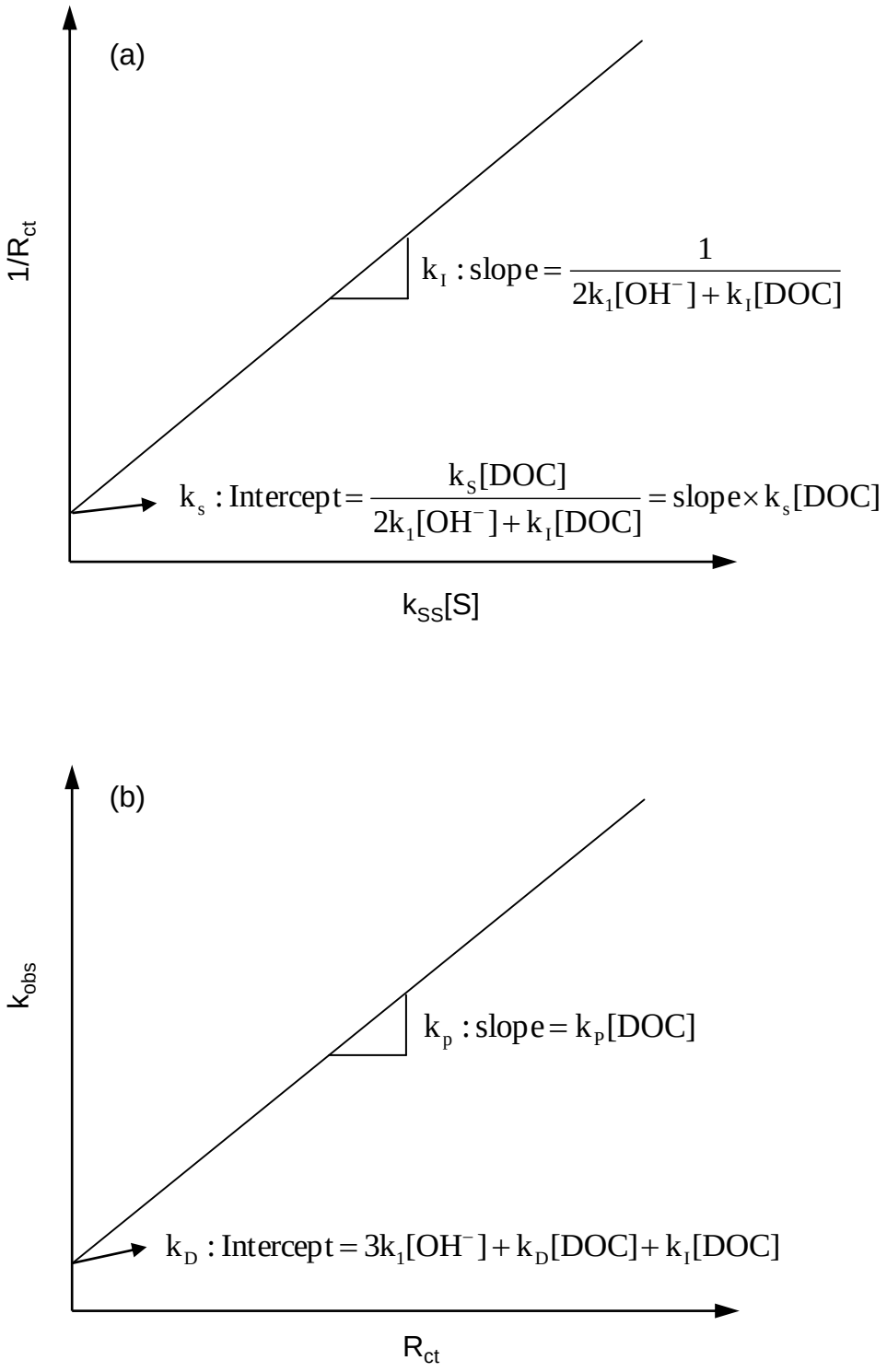

Figure 4.1 The theoretical relationship of (a) $1/R_{ct}$ plotted against ($k_{SS}[S]$) and (b) k_{obs} plotted against R_{ct}.

4.2 Determination of the initiation, inhibition and promotion rate constants for NOM isolates.

Figure 4.2 shows the R_{ct} plots for SRHA, SRFA and SAHA in the presence of different *tert*-butanol concentrations at pH 8.0. For all three NOM isolates, a two-stage R_{ct} pattern was found, which has been commonly observed for the ozonation of natural water [27, 32, 35]. The initial high R_{ct} was believed to be due to the instantaneous formation of ·OH generated from the reaction of fast-reacting initiation functional groups in bulk NOM with ozone. It has been suggested that phenolic and amine moieties in the NOM macromolecule could contribute to the high initial R_{ct} value [37]. Since limited data points (< 3) could be obtained using the standard batch dispenser setup during the short period of the first R_{ct} stage (< 20 s), only the second stage R_{ct} was considered for the determination of initiation (k_I), inhibition (k_S), promotion (k_P) and direct reaction (k_D) rate constants.

In general, the second stage R_{ct} value determined for the three NOM isolates increased with the decreasing *tert*-butanol concentration (Table 4.1), which was consistent with the trend illustrated by Equation (4.1). Figure 4.3 shows the plot of $1/R_{ct}$ vs. $k_{SS}[S]$ for all three NOM isolates, and linear correlations were observed. As shown in Figure 4.1(a), the values of k_I and k_S can be determined from the slope and intercept, respectively, with the known pH value (or $[OH^-]$), k_1 (160 $M^{-1}s^{-1}$ (Section 3.2)), *tert*-butanol concentration ([S]) and k_{SS} (6.0×10^8 $M^{-1}s^{-1}$ [23]). The k_1 value of 160 $M^{-1}s^{-1}$ used here was previously calibrated in Chapter 3 and was within an acceptable range of agreement with the literature values (70 $M^{-1}s^{-1}$ to 220 $M^{-1}s^{-1}$ [27, 82, 85]).

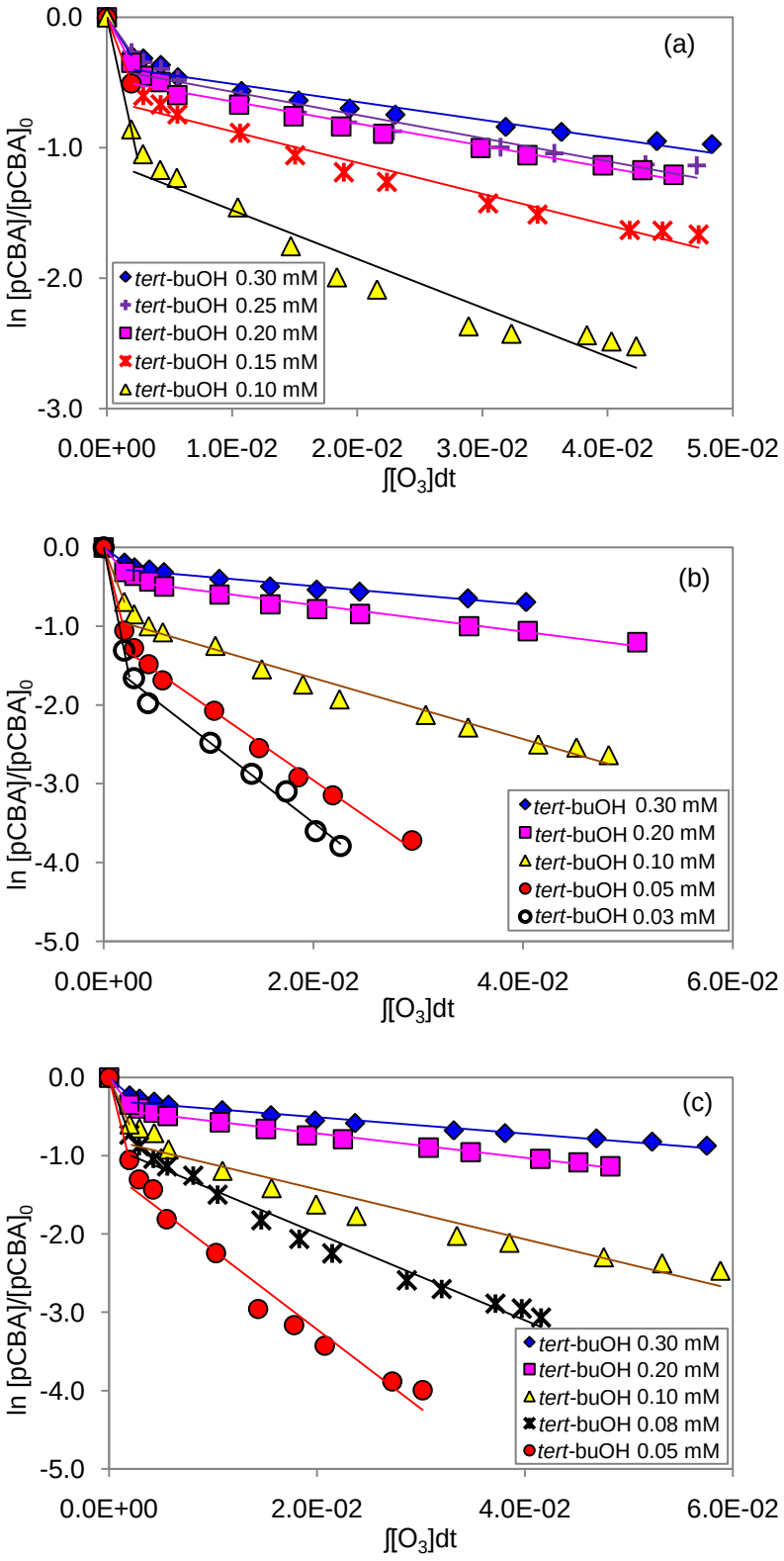

Figure 4.2 The R_{ct} plots for three different NOM isolates, (a) SRHA, (b) SRFA and (c) SAHA, in the presence of different *tert*-butanol concentrations. Experimental conditions: pH 8.0, initial ozone concentration = 0.1 mM, NOM concentration = 2.0 mg/L (approximately 0.9 mg C/L), pCBA = 0.5 µM and phosphate buffer = 1 mM.

Table 4.1 The R_{ct} values determined for the three NOM isolates at different concentrations of *tert*-butanol. Experimental conditions: pH 8.0, initial ozone concentration = 0.1 mM, NOM concentration = 2.0 mg/L, *tert*-butanol = 0.3-0.03 mM, pCBA = 0.5 μM and phosphate buffer = 1 mM.

Tert-butanol (mM)	SRHA R_{ct}	SRFA R_{ct}	SAHA R_{ct}
0.30	$(2.9\pm0.2)\times10^{-9}$	$(2.8\pm0.4)\times10^{-9}$	$(2.8\pm0.1)\times10^{-9}$
0.25	$(3.7\pm0.1)\times10^{-9}$	-	-
0.20	$(4.2\pm0.4)\times10^{-9}$	$(3.9\pm0.2)\times10^{-9}$	$(3.9\pm0.1)\times10^{-9}$
0.15	$(5.8\pm0.2)\times10^{-9}$	-	-
0.10	$(8.9\pm1.3)\times10^{-9}$	$(7.7\pm1.1)\times10^{-9}$	$(7.9\pm0.1)\times10^{-9}$
0.08	-	-	$(9.9\pm0.8)\times10^{-9}$
0.05	-	$(16.2\pm1.0)\times10^{-9}$	$(14.8\pm2.2)\times10^{-9}$
0.03	-	$(23.8\pm5.2)\times10^{-9}$	-

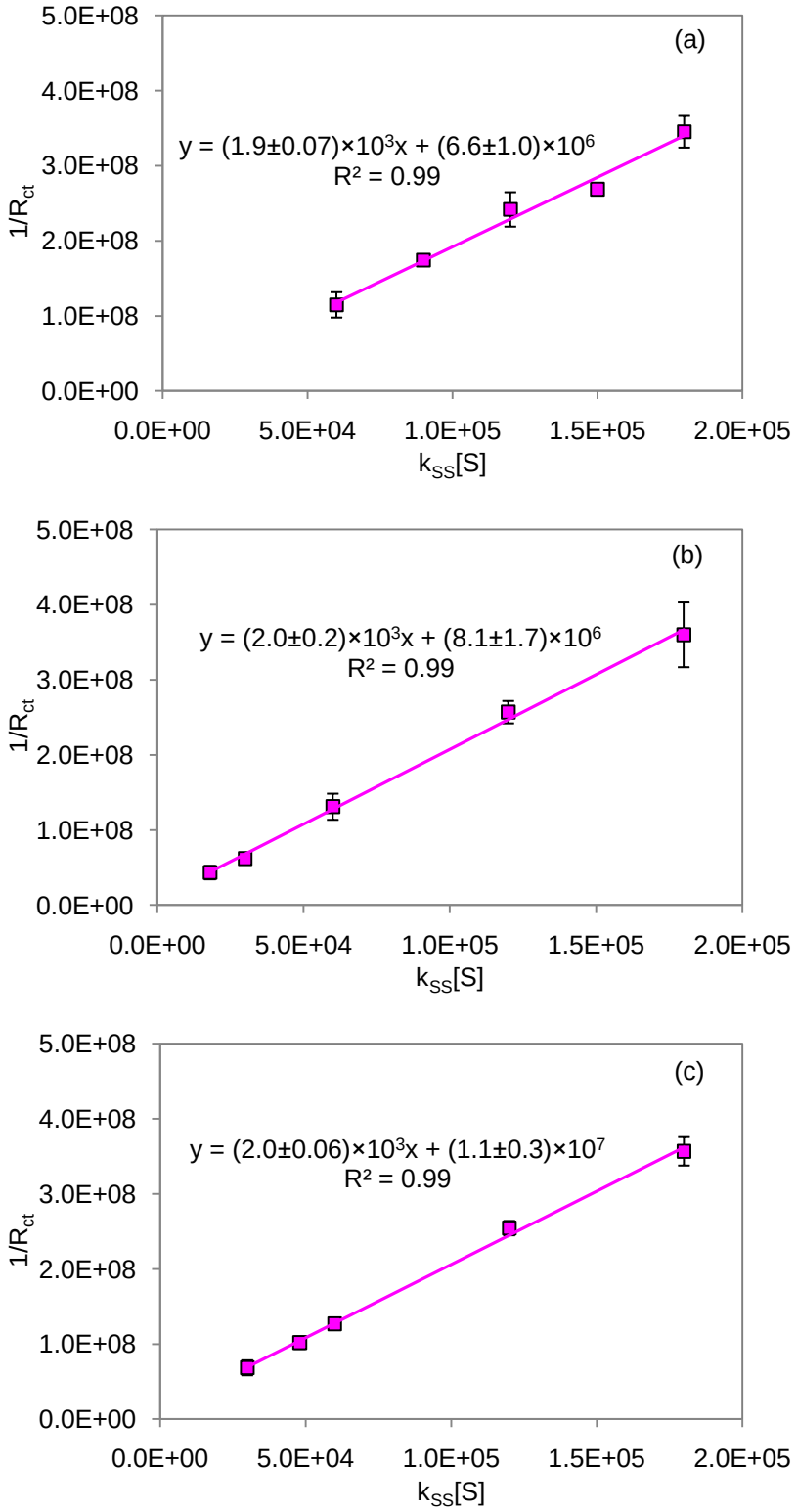

Figure 4.3 The plots of $1/R_{ct}$ vs ($k_{SS}[S]$) for different NOM isolates. (a) SRHA, (b) SRFA and (c) SAHA. Experimental conditions: pH 8.0, initial ozone concentration = 0.1 mM, NOM concentration = 2.0 mg/L (approximately 0.9 mg C/L), *tert*-butanol = 0.03-0.3 mM, pCBA = 0.5 µM and phosphate buffer = 1 mM.

The determined k_I and k_S are presented in Table 4.2. It is interesting to note that similar k_I values were determined for these different NOM isolates, i.e. $(2.4\pm0.2)\times10^{-4}$, $(2.0\pm0.6)\times10^{-4}$ and $(2.2\pm0.2)\times10^{-4}$ L(mg C)$^{-1}$s^{-1} for SRHA, SRFA and SAHA, respectively, suggesting that they possessed similar initiation capacity per mg C/L in spite of their different chemical properties and sources. On the other hand, the k_S values determined for these NOM isolates have wider variations, with the values of $(3.9\pm0.5)\times10^{3}$, $(4.4\pm1.1)\times10^{3}$ and $(6.3\pm1.8)\times10^{3}$ L(mg C)$^{-1}$s^{-1} for SRHA, SRFA and SAHA, respectively. This suggested that the three NOM isolates possessed different reactivity in the termination of ·OH chain reactions. It is believed that a variety of NOM functional groups such as aliphatic alkyls, carboxyls and ketones could potentially contribute to the inhibition properties of NOM [24, 26].

Table 4.2 The second-order rate constants of initiation (k_I), inhibition (k_S), promotion (k_P) and direct ozone reaction (k_D) for NOM isolates. Experimental conditions: Initial ozone concentration = 0.1 mM, NOM concentration = 2.0 mg/L, pH = 8.0, *tert*-butanol = 0.03-0.3 mM, pCBA = 0.5 μM and phosphate buffer = 1 mM. k_1=160$M^{-1}s^{-1}$ was used in the calculations.

NOM	k_I ($\times10^{-4}$) ($L(mg\ C)^{-1}s^{-1}$)	k_S ($\times10^{3}$) ($L(mg\ C)^{-1}s^{-1}$)	k_P ($\times10^{4}$) ($L(mg\ C)^{-1}s^{-1}$)	k_D ($\times10^{-4}$) ($L(mg\ C)^{-1}s^{-1}$)
SRHA	2.4±0.2	3.9±0.5	8.1±1.8	10.7±0.1
SRFA	2.0±0.6	4.4±1.1	7.5±1.4	6.9±1.8
SAHA	2.2±0.2	6.3±1.8	7.2±1.3	7.1±0.7

The decomposition of ozone in all experiments can be described by the pseudo first-order kinetics (Figure 4.4). The plots of k_{obs} vs. R_{ct}, which can be used to determine k_P and k_D, are shown in Figure 4.5. Linear correlations were observed for all three NOM isolates which were consistent with the trend illustrated by Equation (4.3). It should be noted that such linear correlation has also been observed in the ozonation of natural water [36, 88]. As shown in Figure 4.1(b), k_P and k_D can be determined from the slope and intercept of the plot, respectively, and the values obtained are summarized in Table 4.2. The differences of k_P and k_D between the three NOM isolates were relatively small except the higher k_D for SRHA. The direct reaction most likely involved the olefin functional groups of NOM [29] as they can readily react with ozone following the Criegee mechanism with rate constants at the range of 0.1×10^3 to 5.7×10^3 $M^{-1}s^{-1}$ [19, 89]. The functional groups that can contribute to the promotion property of NOM are not clear. However, it is well-established that formic acid and methanol can act as the promoter in ozonation reactions [26]. It is expected that some carboxyl and hydroxyl functional groups in bulk NOM may facilitate the promotion reaction of NOM.

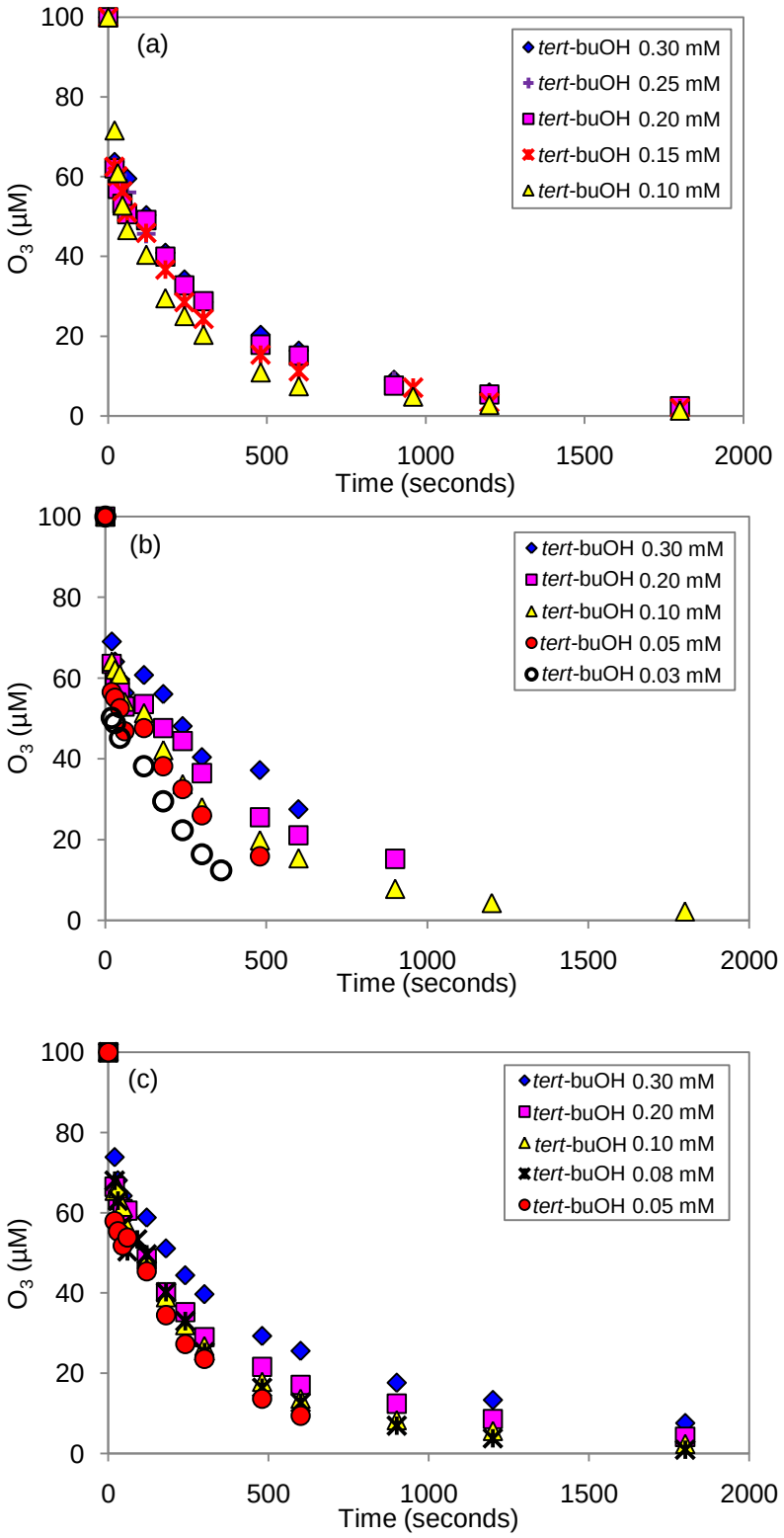

Figure 4.4 The ozone decomposition of three different NOM isolates, (a) SRHA, (b) SRFA and (c) SAHA, at different *tert*-butanol concentrations. Experimental conditions: pH 8.0, initial ozone concentration = 0.1 mM, NOM concentration = 2.0 mg/L (approximately 0.9 mg C/L), pCBA = 0.5 µM and phosphate buffer = 1 mM.

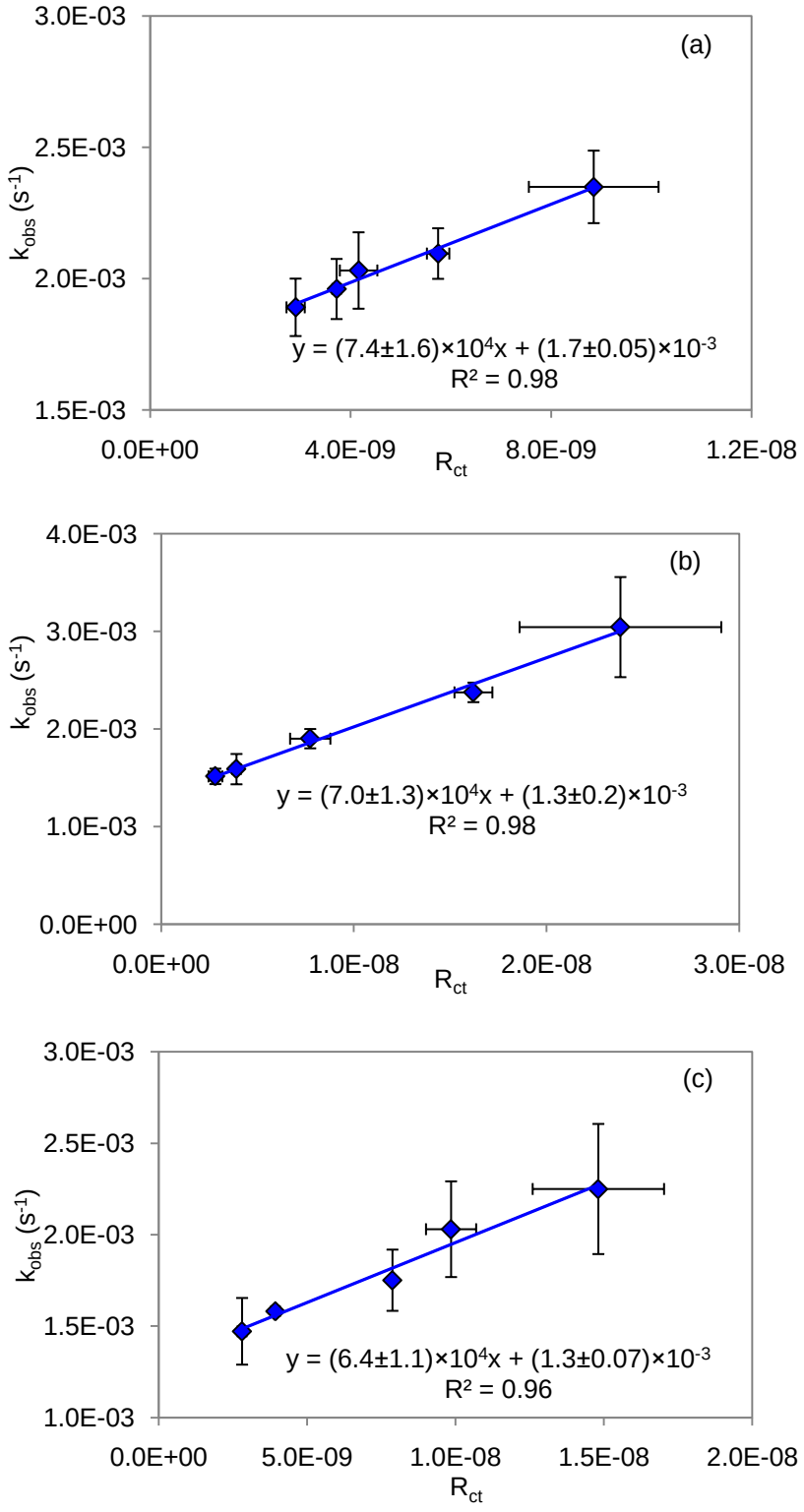

Figure 4.5 The plots of k_{obs} vs. R_{ct} for different NOM isolates. (a) SRHA, (b) SRFA and (c) SAHA. Experimental conditions: pH 8.0, initial ozone concentration = 0.1 mM, NOM concentration = 2.0 mg/L (approximately 0.9 mg C/L), *tert*-butanol = 0.03-0.3 mM, pCBA = 0.5 μM and phosphate buffer = 1 mM. The error bar represents the standard deviation of triplicates.

Since the value of k_1 has been reported to be in the range of 70 $M^{-1}s^{-1}$ to 220 $M^{-1}s^{-1}$ [27, 82, 85], a sensitivity analysis was conducted to evaluate the variability of k_I, k_S, k_P and k_D in response to the change of k_1 and the results are shown in Table 4.3. Based on the developed method, the change of k_1 does not affect the determination of k_p and k_S (see Figure 4.1). The response of k_D to the variation of k_1 (70 $M^{-1}s^{-1}$ to 220 $M^{-1}s^{-1}$) showed that k_D was only slightly affected with deviations of -14.1% and +9.9% from the value determined using k_1 = 160 $M^{-1}s^{-1}$. The response of k_I to the same variation of k_1, on the other hand, showed higher deviations of -95.0% and +65.0%. The value of k_1, thus, should be calibrated for different systems or a lower pH value can be employed to minimize the impact of k_1 by reducing the initiation capacity contributed by OH^-.

Table 4.3 The sensitivity analysis for second-order rate constants for direct ozone reaction (k_D), initiation (k_I), promotion (k_P) and inhibition (k_S) of NOM isolates using k_1 = 70 $M^{-1}s^{-1}$ or 220 $M^{-1}s^{-1}$

NOM	k_I ($\times 10^{-4}$) ($L(mg\ C)^{-1}s^{-1}$)		k_S ($\times 10^{3}$) ($L(mg\ C)^{-1}s^{-1}$)		k_P ($\times 10^{4}$) ($L(mg\ C)^{-1}s^{-1}$)		k_D ($\times 10^{-4}$) ($L(mg\ C)^{-1}s^{-1}$)	
	k_1 = 70	k_1 = 220	k_1 = 70	k_1 = 220	k_1 = 70	k_1 = 220	k_1 = 70	k_1 = 220
SRHA	(4.4 ± 0.2)	(1.1 ± 0.2)	(3.9 ± 0.5)		(8.1 ± 1.8)		(10.8 ± 0.8)	(10.1 ± 0.6)
SRFA	(3.9 ± 0.6)	(0.7 ± 0.6)	(4.4 ± 1.1)		(7.5 ± 1.4)		(7.3 ± 1.2)	(6.3 ± 1.8)
SAHA	(4.2 ± 0.2)	(0.8 ± 0.2)	(6.3 ± 1.8)		(7.2 ± 1.3)		(8.1 ± 0.7)	(6.4 ± 0.7)

The summation of rate constants of the reactions between NOM isolate and ozone, i.e. $k_I + k_D$, for SRHA, SRFA and SAHA were $(13.1\pm0.2)\times10^{-4}$, $(8.9\pm1.8)\times10^{-4}$ and $(9.3\pm0.7)\times10^{-4}$ L(mg C)$^{-1}$s^{-1}, respectively. These values could also be determined experimentally from the pseudo-first order ozone decomposition at high inhibitor concentration (0.5 mM of *tert*-butanol) as shown in Figure 4.6. The high concentration of inhibitor would terminate the ·OH chain reactions propagated by the NOM promotion reaction. To determine the pseudo-first order ozone decomposition rate constant under such conditions, Equation (4.3) is rewritten as the following:

$$-\frac{d[O_3]}{dt}\frac{1}{[O_3]} = k_{obs} = 3k_1[OH^-] + k_D[DOC] + k_I[DOC] \quad (4.4)$$

Thus, $(k_I + k_D)$ can be obtained by rearranging Equation (4.4) :

$$(k_D + k_I) = \frac{(k_{obs} - 3k_1[OH^-])}{[DOC]} \quad (4.5)$$

The experimentally determined values $(k_I + k_D)$, i.e. 12.2×10^{-4}, 7.7×10^{-4} and 6.4×10^{-4} L (mg C)$^{-1}$s^{-1} for SRHA, SRFA and SAHA, respectively, were found to be comparable with those determined using the proposed new method.

The overall ·OH scavenging rate constants, i.e. $k_P + k_S$, for SRHA, SRFA and SAHA were $(8.5\pm1.8)\times10^4$, $(7.9\pm1.4)\times10^4$ and $(7.8\pm1.3)\times10^4$ L(mg C)$^{-1}$s^{-1}, respectively. These values were higher than those determined using pulse radiolysis and ozone-based competition kinetics for NOM isolates collected from different sources (i.e. 1.3×10^4 to 7.3×10^4 L(mg C)$^{-1}$s^{-1} [62, 90-92]) but they had the same order of magnitude.

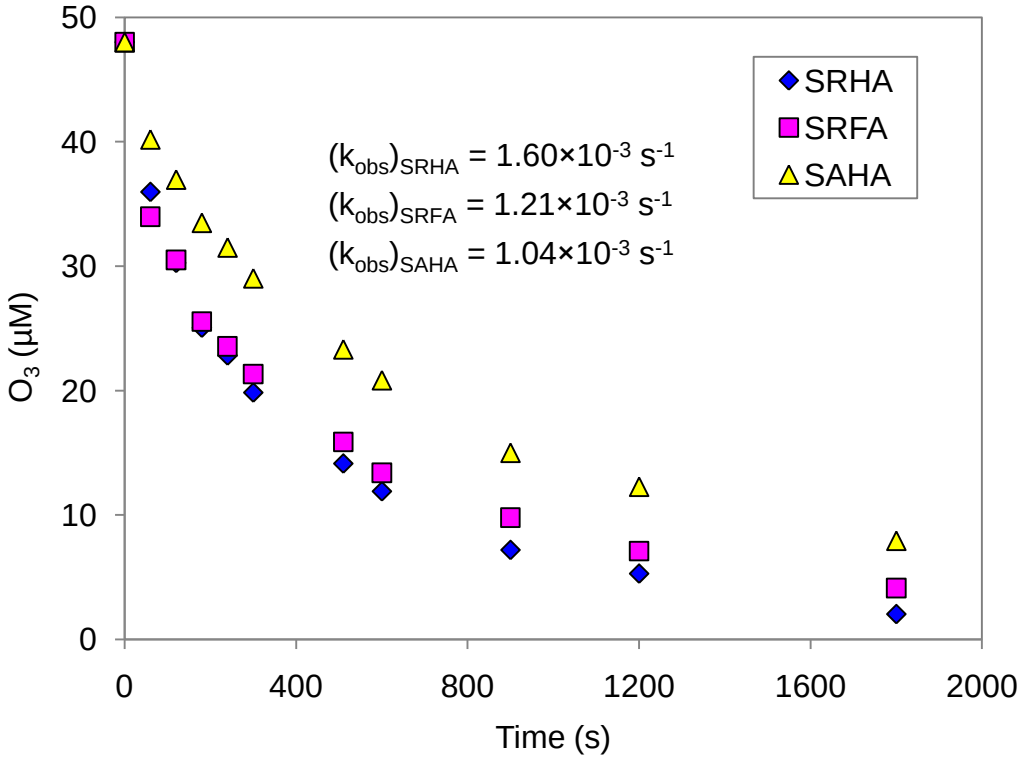

Figure 4.6 Pseudo first-order O_3 decomposition in the presence of different NOM isolates at high *tert*-butanol concentration. Experimental conditions: pH = 8.0, initial ozone concentration = 0.05 mM, *tert*-butanol = 0.5 mM, pCBA = 0.5 µM and phosphate buffer = 1 mM.

4.3 Determination of the initiation, inhibition, promotion and direct reaction rate constants of NOM in natural water

In natural water, the typical species that can significantly affect the R_{ct} value are OH^- (or pH), NOM and carbonate alkalinity (HCO_3^-/CO_3^{2-}) [36]. NOM contributes simultaneously to the initiation, promotion and inhibition in ozonation [26] whereas carbonate alkalinity can only serve as the inhibitor [24]. With the presence of carbonate alkalinity, Equation (4.1) can be expanded to the following:

$$R_{ct} = \frac{2k_1[OH^-] + k_I[DOC]}{k_{SS}[S] + k_S[DOC] + k_{HCO_3^-}[HCO_3^-] + k_{CO_3^{2-}}[CO_3^{2-}]} \quad (4.6)$$

Again, to determine k_I and k_S values, Equation (4.6) is inversed, yielding the following equation:

$$\frac{1}{R_{ct}} = \frac{k_{SS}[S] + k_S[DOC] + k_{HCO_3^-}[HCO_3^-] + k_{CO_3^{2-}}[CO_3^{2-}]}{2k_1[OH^-] + k_I[DOC]} \quad (4.7)$$

The slope and an intercept of a plot of $1/R_{ct}$ vs. $k_{ss}[S]$ would become $\frac{1}{(2k_1[OH^-] + k_I[DOC])}$ and $\frac{(k_S[DOC] + k_{HCO_3^-}[HCO_3^-] + k_{CO_3^{2-}}[CO_3^{2-}])}{(2k_1[OH^-] + k_I[DOC])}$, respectively. The total initiation capacity $(2k_1[OH^-] + k_I[DOC])$ and the total inhibition capacity $(k_S[DOC] + k_{HCO_3^-}[HCO_3^-] + k_{CO_3^{2-}}[CO_3^{2-}])$ of the natural water can then be determined from the slope and intercept, respectively. For the quantification of k_P and k_D values, no changes should be made on Equation (4.3) as bicarbonate and carbonate ions possess low reactivity with ozone (< 1 $M^{-1}s^{-1}$ [93]).

The applicability of the proposed method to NOM in natural water was demonstrated using a reservoir water collected in Singapore. The R_{ct} plots obtained from the ozonation of the water with the addition of different *tert*-butanol concentrations are shown in Figure 4.7. Similar to the R_{ct} plots observed in the NOM isolates (Figure 4.2), the two-stage R_{ct} pattern was observed for all *tert*-butanol concentrations employed [27, 36]. As discussed in Section 4.2, the phenols and amines moieties in the NOM structure are responsible for the initial high R_{ct} stage [37]. These moieties are present in limited quantities within bulk NOM and could be quickly consumed in the ozonation process, resulting in a smaller R_{ct} value in the second stage.

Figure 4.8(a) shows the plot of 1/ R_{ct} vs. $k_{SS}[S]$. A linear correlation with a slope of 3.5×10^{3} and an intercept of 7.3×10^{7} was observed. The total initiation and inhibition capacities of the water were determined to be 2.0×10^{-4} s^{-1} and 2.1×10^{4} s^{-1} from the slope and intercept, respectively. Considering that the initiation capacity was contributed primarily by OH^- and DOC, k_I for this reservoir NOM can be determined by subtracting the initiation capacity of OH^- ($k_1[OH^-]$) from the total initiation capacity. Similarly, k_S for this reservoir NOM can be determined by subtracting the inhibition capacity of carbonate alkalinity (7.0×10^{3} s^{-1}) from the total inhibition capacity. The k_I and k_s of this reservoir NOM were calculated to be 8.8×10^{-5} L (mg C)$^{-1}s^{-1}$ and 5.9×10^{3} L (mg C)$^{-1}s^{-1}$, respectively.

The promotion and direct reaction rate constants of NOM was quantified using the slope (8.9×10^{4}) and intercept (1.3×10^{-3}) of the plot of k_{obs} vs. R_{ct} (Figure 4.8(b)), respectively. The k_P value was determined to be 3.9×10^{4} L (mg C)$^{-1}s^{-1}$. According to Figure 4.1(b), the intercept is contributed by the OH^- initiation capacity as well as the initiation and direct reaction capacities of the reservoir NOM. Subtracting the OH^-

and NOM initiation capacities from the intercept resulted in a value of 8.9×10^{4} s^{-1} which represented the total direct reaction capacity of the reservoir NOM. Therefore, the k_D value of the reservoir NOM was determined to be 4.2×10^{-4} L (mg C)$^{-1}s^{-1}$.

With the determined rate constants of NOM, the R_{ct} value resulting from the ozonation of this reservoir water can be modeled using the following equation (Equation (4.6) without the contribution of *tert*-butanol):

$$R_{ct} = \frac{2k_I[OH^-] + k_I[DOC]}{k_S[DOC] + k_{HCO_3^-}[HCO_3^-] + k_{CO_3^{2-}}[CO_3^{2-}]} = \frac{320\times[OH^-] + 8.8\times10^{-5}[DOC]}{5.9\times10^{3}[DOC] + 8.5\times10^{6}[HCO_3^-] + 4\times10^{8}[CO_3^{2-}]} \quad (4.8)$$

The influences of pH value and carbonate alkalinity on the R_{ct} value can be simulated using Equation (4.8) as shown in Figure 4.9. The R_{ct} value increases at a faster rate as the pH increases (Figure 4.9(a)). This trend is due to the decreasing significance of NOM initiation relative to the total initiation capacity with increasing pH. As for the influence of carbonate alkalinity, the R_{ct} value would gradually decrease to an asymptote with the increasing carbonate alkalinity (Figure 4.9(b)). This trend is due to the nature of Equation (4.8) and the decreasing significance of NOM inhibition to the total inhibition capacity as the carbonate alkalinity increases. These trends of R_{ct} change as a function of pH value and carbonate alkalinity in the ozonation of natural water have been observed in previous study but could not be fully explained [36]. These trends can be explained by the new R_{ct} equation (Equation (3.1) or (4.8)) and the unique contribution of NOM to the R_{ct}. It should be noted that the values of k_I and k_s for NOM could potentially vary as a function of pH due to the deprotonation of carboxyl and phenolic functional groups. The variations, however, are expected to be minor at the typical pH values (pH 6.0-9.0) found in natural water due to the relatively constant charge density of NOM at this pH range [94].

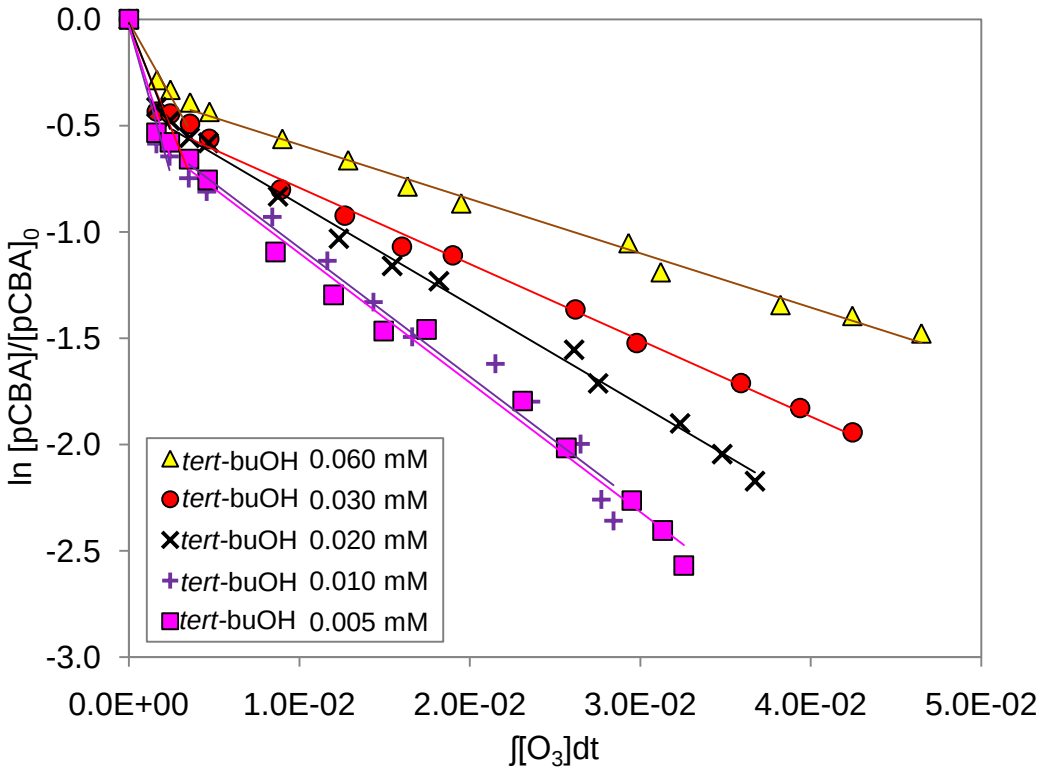

Figure 4.7 The R_{ct} plot of the natural water ozonation in the presence of different *tert*-butanol concentrations. Experimental conditions: pH 7.4, initial ozone concentration = 83 µM, DOC = 2.3 mg/L, alkalinity = 39 mg/L as $CaCO_3$, pCBA = 0.5 µM and phosphate buffer = 1 mM.

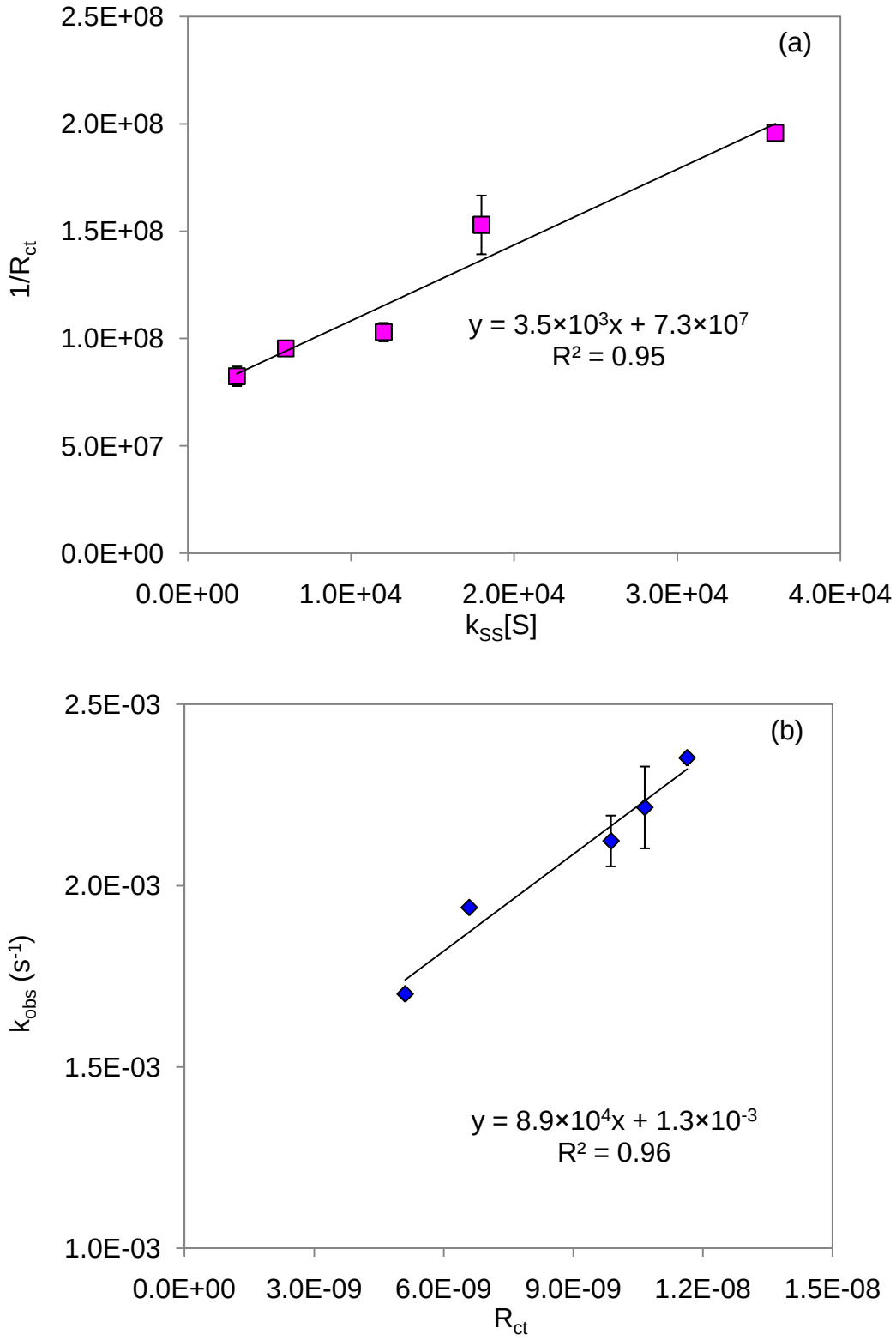

Figure 4.8 Ozonation of natural water in the presence of different *tert*-butanol concentrations (a) $1/R_{ct}$ vs. $k_{SS}[S]$ plot and (b) k_{obs} vs. R_{ct} plot. Experimental conditions: pH 7.4, initial ozone concentration = 83 µM, DOC = 2.3 mg/L, alkalinity = 39 mg/L as $CaCO_3$, pCBA = 0.5 µM and phosphate buffer = 1 mM.

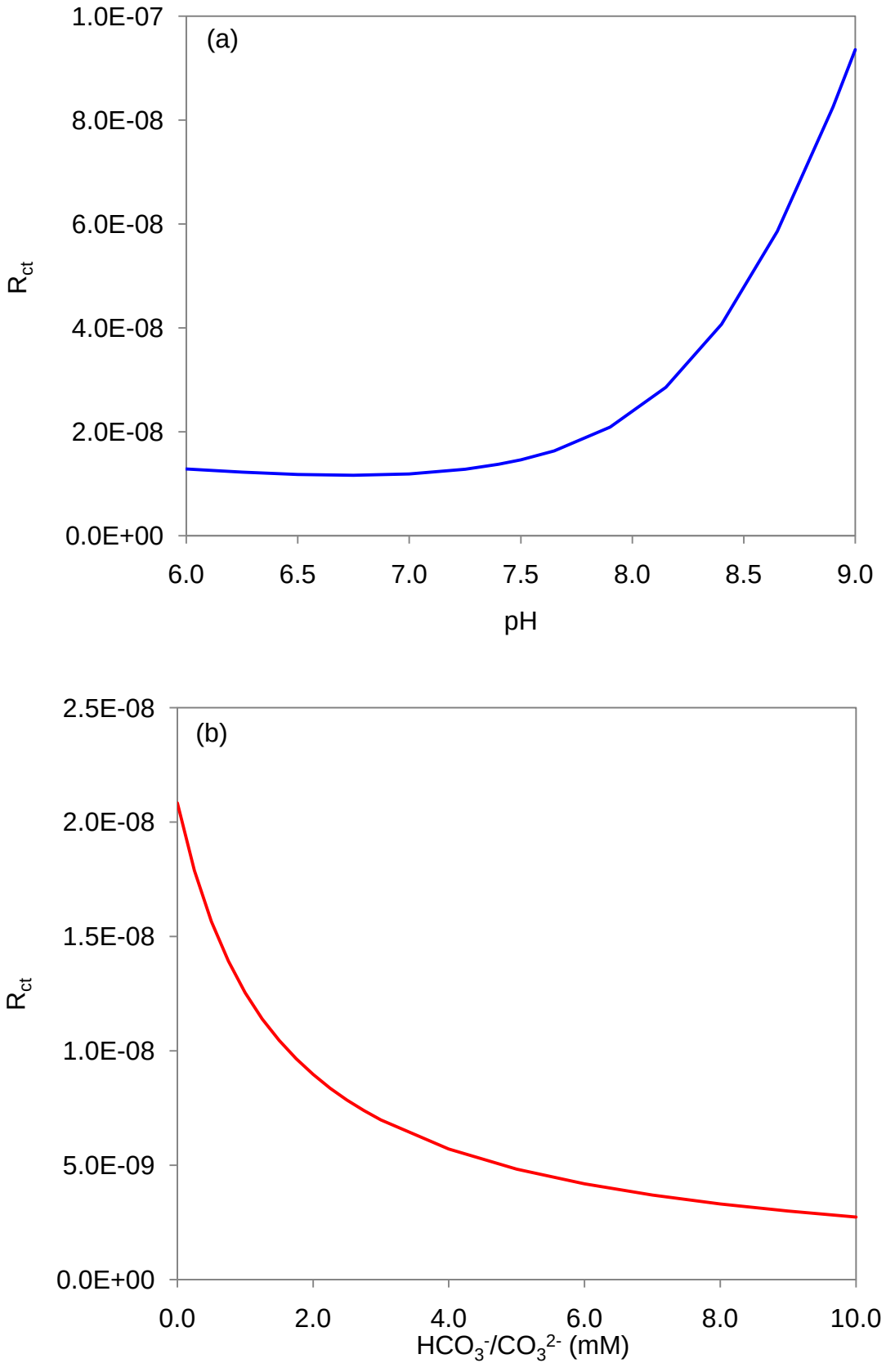

Figure 4.9 Model simulation of R_{ct} value for the reservoir water as a function of (a) pH and (b) carbonate alkalinity.

4.4 Conclusions

The application of the proposed new method to determine the rate constants of NOM as the initiator, promoter, and inhibitor as well as the direct reaction with ozone is demonstrated in this chapter. With the addition of an external inhibitor, the initiation and inhibition rate constants of NOM can be determined from the slope and intercept of the plot of $1/R_{ct}$ vs. the external inhibition capacity, respectively. The promotion and direct reaction rate constants of NOM can be quantified via the slope and intercept of the plot of pseudo first-order ozone decomposition rate constant vs. R_{ct}, respectively. The applicability of the proposed method was successfully demonstrated using three NOM isolates and a natural water. These findings are crucial in determining the influences of NOM on the removal of organic pollutants, such as pharmaceutical compounds, by water ozonation.

CHAPTER 5

MODELING THE INFLUENCES OF NOM ON THE REMOVAL OF IBUPROFEN DURING WATER OZONATION

The influences of the initiation, promotion and inhibition reactions of NOM on the degradation of an organic pollutant by ozonation could be quantitatively described using the NOM rate constants determined from the proposed method presented in Chapter 4. In this chapter, the influences of the NOM rate constants on the degradation of ibuprofen were investigated using SRFA as the model NOM in the presence of carbonate alkalinity. A discussion on the possible influences of NOM on the removal of other pharmaceutical and organic compounds using results obtained from model simulations was also included in this chapter.

5.1 Modeling the influences of NOM on the degradation of ibuprofen by ozonation

Ibuprofen is a commonly detected pharmaceutical compound in water bodies [67-73]. It possesses a high reactivity toward ·OH ($k_{OH/P} = (7.4\pm1.2)\times10^9$ $M^{-1}s^{-1}$) but reacts slowly with O_3 ($k_{O3/P} = 9.6\pm1$ $M^{-1}s^{-1}$) [77]. Both HCO_3^- and CO_3^{2-} in the carbonate alkalinity act as the inhibitor in water ozonation [24].

As shown in Chapter 4, the first stage R_{ct} observed was always higher than the second stage R_{ct}, and this decrease can significantly affect the level of transient ·OH concentration for the removal of the target organic contaminant. Therefore, the degradation of ibuprofen was investigated in two conditions: 1. ibuprofen was added at the beginning of the reaction when the ozonation was initiated, so that it was

removed in both the first and second R_{ct} stages, and 2. ibuprofen was added 70 s after the ozonation was initiated, so that it was removed only in the second R_{ct} stage.

Figure 5.1 shows the experimental data obtained for both conditions at pH 7.0 in the presence of 0, 2.0 and 4.0 mg/L of SRFA. Because of the time lag of the ibuprofen addition in condition 2, the "reaction time" for ibuprofen was used as the x-axis to allow the easy comparison of experimental data. The ozone concentration at "ibuprofen reaction time = 0" thus differed in these two conditions. In condition 1, the ozone concentration was 100 μM, whereas in condition 2, it was 64 μM and 55 μM for 2.0 and 4.0 mg/L of SRFA, respectively. It was found that the presence of SRFA enhanced ibuprofen removal in both conditions and that the enhancement was more pronounced in condition 1. The high transient ·OH exposure resulting from the first stage R_{ct} should have played a major role in the ibuprofen removal [37].

The degradation of ibuprofen can be modeled by substituting Equation (4.8) into Equation (1.12) to yield the following equation:

$$\ln\left(\frac{[P]}{[P]_0}\right) = -\left(\int [O_3]dt\right)\left(k_{\cdot OH/P}\left(\frac{2k_I[OH^-] + k_I[DOC]}{k_S[DOC] + k_{HCO_3^-}[HCO_3^-] + k_{CO_3^{2-}}[CO_3^{2-}]}\right) + k_{O_3/P}\right) \quad (5.1)$$

Equation (5.1) indicates that the factors that affect the removal of ibuprofen include ozone exposure, the OH^- initiation capacity (or the pH value), the SRFA initiation and inhibition capacities and the carbonate alkalinity inhibition capacity.

The simulated ibuprofen degradation, represented by dotted lines, using Equation (5.1) is shown in Figure 5.1. The simulated values agreed reasonably well with the experimental data obtained for condition 2 but underestimated those obtained for condition 1. This was expected because the rate constants of SRFA used in the

simulation were determined from the second R_{ct} stage. Both experimental and simulated results showed that the SRFA concentration does not significantly affect the removal of ibuprofen. By careful examination of the different roles of SRFA in the ozonation process, several facts can be deduced. Firstly, when the SRFA concentration was increased from 2.0 to 4.0 mg/L, the inhibition capacity, contributed by SRFA, increased from 4.1×10^{3} s^{-1} to 8.2×10^{3} s^{-1}. However, the total inhibition capacity for both conditions only differed slightly (1.9×10^{4} s^{-1} vs. 2.3×10^{4} s^{-1} for conditions 1 and 2, respectively) due to the dominant contribution from the carbonate alkalinity (1.5×10^{4} s^{-1}). Thus, the influence of SRFA inhibition on the degradation of ibuprofen for the two concentrations employed was relatively insignificant. Secondly, the initiation capacities contributed by 2.0 and 4.0 mg/L of SRFA were 1.9×10^{-4} s^{-1} and 3.8×10^{-4} s^{-1}, respectively. These initiation capacities were about 6 and 12 times higher than that contributed by OH^{-} at pH 7.0 (3.2×10^{-5} s^{-1}), suggesting that the initiation moieties of SRFA played an important role in the degradation of ibuprofen. Finally, the increase in the SRFA concentration would accelerate the direct reaction and enhance the promotion capacity that could significantly affect the ozone exposure.

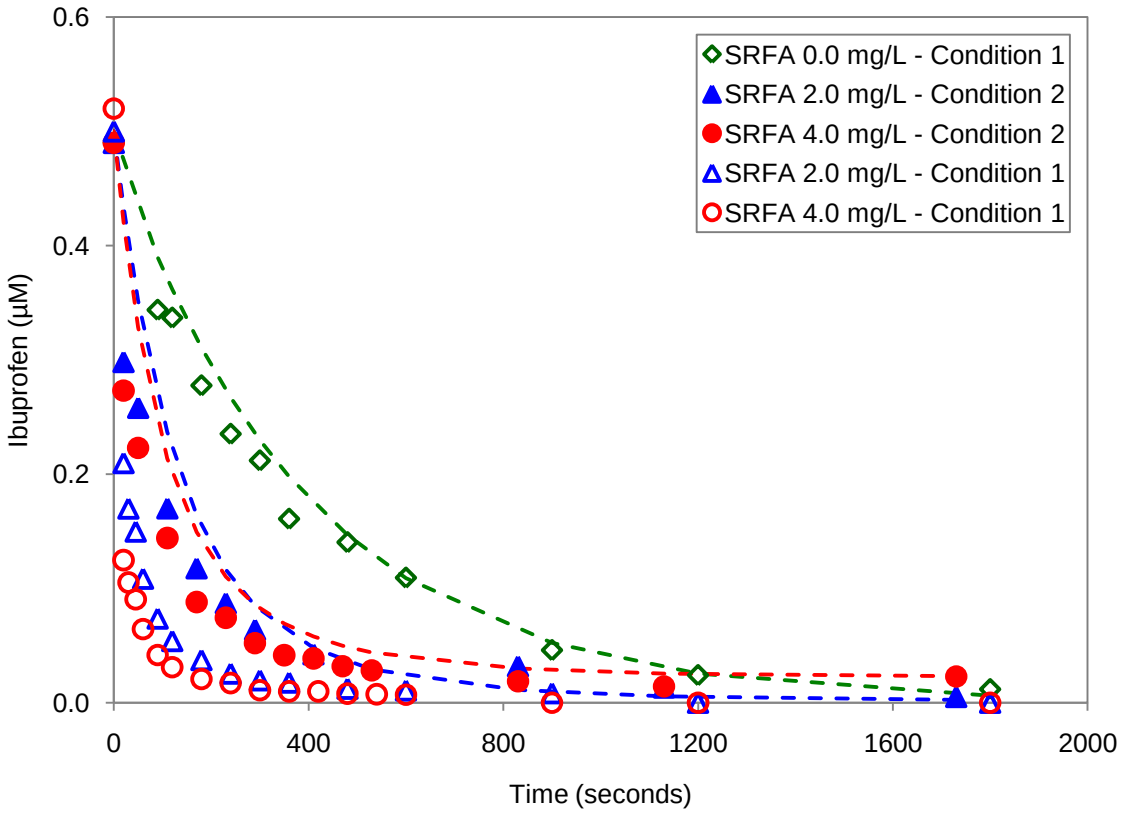

Figure 5.1 Effects of SRFA concentration (0-4.0 mg/L) on the degradation of ibuprofen. Open symbol: ibuprofen was added at the beginning of ozonation (condition 1); Solid symbol: ibuprofen was added after 70 s of ozonation (condition 2); dashed lines: model prediction. Experimental conditions: pH 7.0, initial ozone concentration = 0.1 mM, carbonate alkalinity = 2 mM, ibuprofen = 0.5 μM, pCBA = 0.5 μM and phosphate buffer = 1 mM.

Figure 5.2 shows the experimental ozone and ·OH exposures and those calculated using Equations (1.8), (1.13) and (4.8) after 110 s (Figure 5.2(a)) and 290 s (Figure 5.2(b)) of ibuprofen "reaction time". At 110 s, the measured ozone exposure was reduced from 11.6×10^{-3} M·s to 6.7×10^{-3} M·s and 5.4×10^{-3} M·s with the addition of 2.0 and 4.0 mg/L SRFA, respectively. The measured ·OH exposure, on the other hand, increased from 2.7×10^{-11} M·s to 5.8×10^{-11} M·s and 7.1×10^{-11} M·s. The simulated results were in good agreements with the observed values. Similar trends were found for ozone and ·OH exposures at 290 s. Because the removal of ibuprofen in the system depended on the total oxidation capacity, i.e., $k_{O_3/P}\left(\int[O_3]dt\right) + k_{\cdot OH/P}\left(\int[\cdot OH]dt\right)$, the "trade-off" between the loss of ozone oxidation capacity and the gain of ·OH oxidation capacity resulted in similar ibuprofen removal in the two SRFA concentrations. In contrast, the results obtained in the absence of SRFA showed a significant decrease between the exposures of ozone and ·OH. A breakdown of the contributions of OH^- and different reaction modes of SRFA to k_{obs} (Equation (4.3)) showed that the main contributors to the decomposition of ozone in our experiments were $k_p[DOC]\times R_{ct}$ and $k_D[DOC]$, which together accounted for more than 86 % of ozone decomposition (Table 5.1). The increase in SRFA concentration, however, did not significantly affect its contribution as initiator, promoter and inhibitor to k_{obs}.

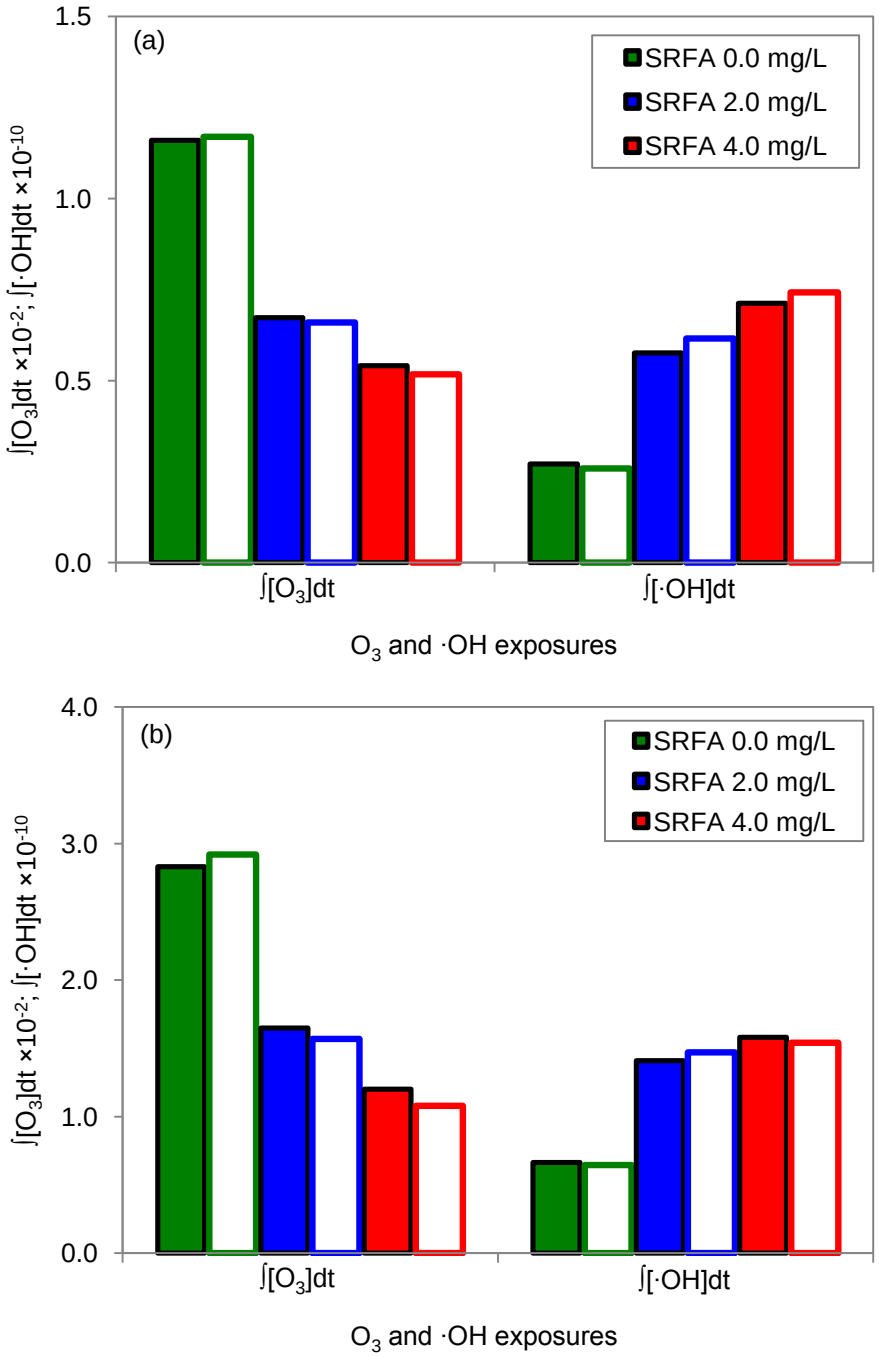

Figure 5.2 O_3 and ·OH exposures for ibuprofen in the presence of 0, 2.0 and 4.0 mg/L of SRFA after different reaction times of (a) 110 s and (b) 290 s. The solid bar represents the experimentally determined exposure, whereas the open bar represents the modeled exposure. Experimental conditions: Initial ozone concentration = 0.1 mM, HCO_3^-/CO_3^{2-} = 2 mM, ibuprofen = 0.5 µM, pCBA = 0.5 µM and phosphate buffer = 1 mM. In the presence of SRFA, ibuprofen was added 70 s after ozonation was initiated.

Table 5.1 The contributions of OH^- and different reaction modes of SRFA to the ozone decomposition rate constant (k_{obs}).

	Contribution to k_{obs} (%)	
	SRFA 2.0 mg/L	SRFA 4.0 mg/L
$3k_I[OH^-]$	2.8	1.3
$k_D[DOC]$	37.8	34.3
$k_I[DOC]$	11.0	9.9
$k_P[DOC]\times R_{ct}$	48.5	54.5

5.2 Application of the model to other pharmaceutical and organic compounds

The presence of NOM may not always enhance the removal of pharmaceutical and organic compounds as it depends on the total oxidation capacity contributed by both ozone and ·OH. Typically, organic contaminants possess second-order rate constants in the reaction with ·OH in the order of 10^9 $M^{-1}s^{-1}$ but in the reaction with O_3, however, it can vary widely by several orders of magnitude. Here, the removal of six different organic compounds in the presence of 0, 2 and 4 mg/L SRFA was modeled, including five pharmaceutical compounds (diazepam, N(4)-acetylsulfamethoxazole, bezafibrate, metoprolol and penicillin G) and a pulp bleach (zinc diethylenediamintetraacetate), which have all been detected in surface waters [67, 68, 69, 71, 95, 96]. These compounds were selected because they possess highly different rate constants with ozone but possess comparable rate constants in the reaction with ·OH as shown in Table 5.2. SRFA was chosen to model the compounds degradation because it was found to dominate the hydrophobic fraction of NOM [51]. The modeling results were shown in Figure 5.3 and the influences of SRFA on the removal of the compounds are summarized in Table 5.2. It should be noted again that these results represent the removal in the second R_{ct} stage. The simulations indicated that the removal of diazepam (Figure 5.3(a)) in the presence of SRFA was similar to that of ibuprofen. Due to the slow reaction of ozone with diazepam, SRFA generally assisted its removal although a larger difference in removal between 2.0 and 4.0 mg/L SRFA was predicted. On the other hand, Figure 5.3(b) shows that the presence of SRFA impeded the removal of zinc diethylenediamintetraacetate when the $k_{O_3/P}$ increased to 100 $M^{-1}s^{-1}$. The removal of N(4)-acetylsulfamethoxazole illustrated in Figure 5.3(c) was slightly enhanced by SRFA in the first 200 s but was impeded for the subsequent 800 s. The degradation of bezafibrate (Figure 5.3(d)) was also

impeded by SRFA after 100 s of ozonation but SRFA did not affect its removal before the impedance occurred. For metoprolol (Figure 5.3(e)) and penicillin G (Figure 5.3(f)), the presence of SRFA did not affect their removal, primarily due to their high $k_{O_3/P}$. Again, the trade-off between ozone oxidation capacity and ·OH oxidation capacity resulted in a differing influence of SRFA on the removal of these compounds, which can be calculated using their rate constants in the reaction with O_3 and ·OH and the SRFA rate constants, determined from our approach.

Table 5.2 Influences of SRFA on the removal of selected pharmaceutical and organic compounds.

Compound	References	$k_{O_3/P}$ ($M^{-1}s^{-1}$)	$k_{\cdot OH/P}$ ($M^{-1}s^{-1}$)	Impact of NOM
Diazepam	[77]	(0.8±0.2)	$(7.2\pm1.0)\times10^9$	+
Zinc diethylenediamintetraacetate	[97]	100	$(2.4\pm0.4)\times10^9$	–
N(4)-acetylsulfamethoxazole	[98]	250	$(6.8\pm0.1)\times10^9$	+ (< 200 s)
				– (> 200 s)
Bezafibrate	[77]	(590 ±50)	$(7.4\pm1.2)\times10^9$	× (< 100 s)
				– (> 100 s)
Metoprolol	[99, 100]	1.4×10^3	$(8.4\pm0.1)\times10^9$	×
Penicillin G	[98]	4.8×10^3	$(7.3\pm0.3)\times10^9$	×

Note: +: enhance removal efficiency; – : inhibit removal efficiency; ×: no effect in removal efficiency

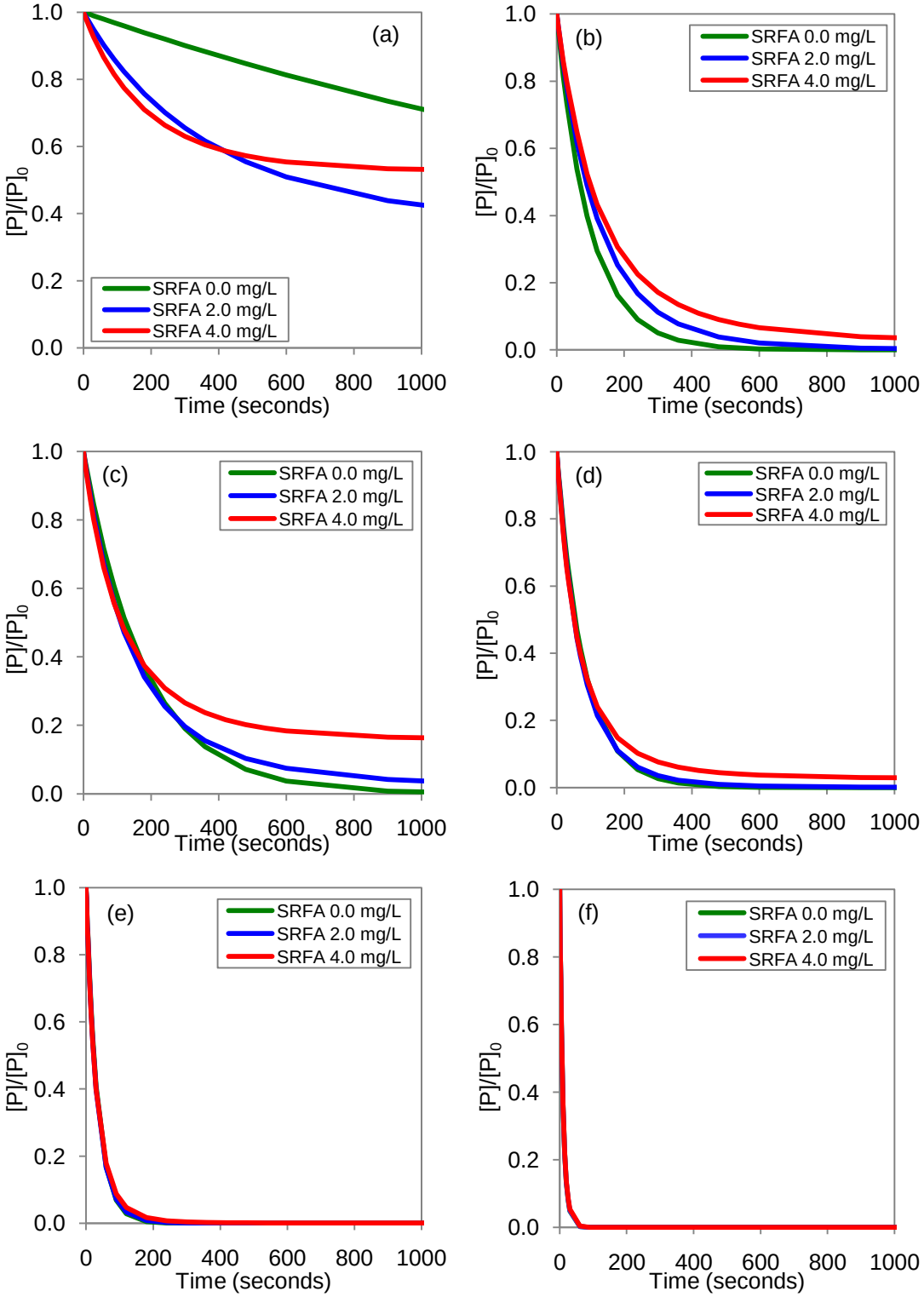

Figure 5.3 Simulation of the removal of selected pharmaceutical and organic compounds, (a) diazepam, (b) zinc diethylenediamintetraacetate, (c) N(4)-acetyl-sulfamethoxazole, (d) bezafibrate, (e) metoprolol and (f) penicillin G, in the presence of 0, 2.0 and 4.0 mg/L SRFA. Ozonation conditions: pH 7.0, initial ozone concentration = 0.021 mM, carbonate alkalinity = 2 mM.

5.3 Conclusions

The influences of NOM on the degradation of ibuprofen in the presence of carbonate alkalinity were quantitatively described using the calculated rate constants of NOM. The experimental and simulated results revealed that the presence of NOM generally enhanced the degradation of ibuprofen due to the initiation moiety of NOM. However, the influence of NOM inhibition moiety was relatively insignificant in the presence of carbonate alkalinity. Because NOM promotion and direct reaction moieties could significantly affect the ozone exposure, the overall removal of ibuprofen was dependent on the total oxidation capacity in the system. With the known rate constants of NOM and reaction rate of organic compounds with O_3 and ·OH, the removal of organic compounds in the presence of NOM can be predicted.

CHAPTER 6

CONCLUSIONS, RECOMMENDATIONS AND FUTURE STUDIES

6.1 Conclusions

In this thesis, a new method that can be used to quantify the reaction rate constants of NOM as the initiator, promoter and inhibitor was developed and validated using representative model compounds. The applicability of the method was demonstrated using three NOM isolates in synthetic solutions and NOM in a natural water. The influences of these different reaction modes of NOM on the removal of ibuprofen by ozonation were determined and modeled. The conclusions of this thesis are summarized as below:

1. The integration of the $^{\bullet}OH$ transient steady-state model and the R_{ct} concept, revealed that R_{ct} value is not only the ratio of $^{\bullet}OH$ exposure to ozone exposure but also the ratio of the initiation capacity to the inhibition capacity of the ozonation system. The R_{ct} value is also linearly correlated with the pseudo-first order ozone decomposition rate constant.
2. With the addition of different concentrations of an external inhibitor to an ozonation system simultaneously containing initiator, promoter and inhibitor, the initiation and inhibition rate constants can be determined from the slope and intercept of the plot of $1/R_{ct}$ vs. the external inhibition capacity, respectively. The promotion rate constant can be determined from the slope of the pseudo first-order ozone decomposition rate constant vs. R_{ct} plot. The method was successfully validated using model compounds that are representative of initiator, promoter and inhibitor, respectively.

3. DOC, a surrogate measurement for the NOM concentration, was incorporated into the proposed method to quantify the initiation, promotion and inhibition rate constants of NOM. The new method was successfully applied to determine these rate constants of three NOM isolates and NOM in a natural water.
4. The determined rate constants of NOM can be used to quantitatively describe the influences of NOM on the degradation of ibuprofen by ozonation. The NOM initiation moiety can greatly improve ibuprofen removal at the initial stage (< 20 s). The significance of the inhibition induced by NOM may depend on the level of carbonate alkalinity present in the water. The promotion and direct reaction of NOM can significantly affect the ozone and $^{\cdot}OH$ exposure that ultimately affect the overall removal of ibuprofen.

6.2 Recommendations

Based on the findings presented in this thesis, recommendations that may benefit the water industry are as follows:

1. The method developed in this study can be used to experimentally quantify the initiation, promotion, inhibition and direct reaction rate constants of NOM. These rate constants can be determined by water treatment utilities using simple batch experiments.
2. With the known rate constants of NOM and the typical water quality parameters, e.g. the pH value and carbonate alkalinity, the removal

efficiency of a target organic compound can be modeled. This may benefit the water utilities in designing an efficient ozonation treatment system.

3. NOM initiation reaction can significantly enhance the removal of ·OH-reactive organic compounds at the initial stage (< 20 s) via the production of higher ·OH concentration. However, the overall removal of these compounds is still dependent on the promotion and direct reactions of NOM. Based on the determined rate constants of NOM using the proposed method, water utilities may be able to predict the total oxidation capacity contributed by both ozone and ·OH and subsequently effective ozone dosage required for their removal.

6.3 Future studies

1. The effects of pH and temperature on the rate constants of NOM need to be evaluated using the proposed method to provide more insights on the potential impacts of these parameters on these rate constants and their influences on the removal of organic contaminants.
2. The rate constants of NOM in the first 20 s were not determined due to the limitations of the experimental setup used in this study. Similar investigations using a quench-flow system are warranted to determine these rate constants of NOM in the initial phase of ozonation and to describe their influences on the removal of organic contaminants of < 20 s.
3. Current investigation only focuses on ibuprofen, an ·OH-reactive organic compound. The degradation of both ·OH- and ozone-reactive organic

compounds as simulated in Chapter 5 should be experimentally investigated.

4. In this study, experiments were conducted in batch reactor. The extension of the study using semi-batch reactor may provide information required for its application in real water treatment plants.
5. The proposed method may also be used to determine the initiation, promotion and inhibition rate constants of wastewater effluent organic matter and their influences on the removal of organic contaminants in wastewater if ozone is employed as a tertiary treatment process.

REFERENCES

1. Rice, R. G., Ozone in the United States of America - State-of-the-art. *Ozone Sci. Eng.* **1999,** *21* (2), 99-118.

2. Larocque, R. L., Ozone applications in Canada - A state of the art review. *Ozone Sci. Eng.* **1999,** *21* (2), 119-125.

3. Geering, F., Ozone applications - The state-of-the-art in Switzerland. *Ozone Sci. Eng.* **1999,** *21* (2), 187-200.

4. Hunt, N. K.; Marinas, B. J., Kinetics of Escherichia coli inactivation with ozone. *Water Res.* **1997,** *31* (6), 1355-1362.

5. Rennecker, J. L.; Marinas, B. J.; Owens, J. H.; Rice, E. W., Inactivation of Cryptosporidium parvum oocysts with ozone. *Water Res.* **1999,** *33* (11), 2481-2488.

6. Driedger, A.; Staub, E.; Pinkernell, U.; Marinas, B.; Koster, W.; von Gunten, U., Inactivation of Bacillus subtilis spores and formation of bromate during ozonation. *Water Res.* **2001,** *35* (12), 2950-2960.

7. Labatiuk, C. W.; Belosevic, M.; Finch, G. R., Factors influencing the infectivity of Giardia-muris cysts following ozone inactivation in laboratory and natural waters. *Water Res.* **1992,** *26* (6), 733-743.

8. Tyrrell, S. A.; Rippey, S. R.; Watkins, W. D., Inactivation of bacterial and viral indicators in secondary sewage effluents, using chlorine and ozone. *Water Res.* **1995,** *29* (11), 2483-2490.

9. Glaze, W. H., Drinking water treatment with ozone. *Environ. Sci. Technol.* **1987,** *21* (3), 224-230.

10. Acero, J. L.; Stemmler, K.; von Gunten, U., Degradation kinetics of atrazine and its degradation products with ozone and OH radicals: A predictive tool for drinking water treatment. *Environ. Sci. Technol.* **2000,** *34* (4), 591-597.

11. Rice, R. G.; Bollyky, L. J.; W.J., L., *Analytical Aspects of Ozone Treatment of Water and Wastewater*. Lewis Publishers: USA, 1986.

12. Langlais, B.; Reckhow, D. A.; Brink, D. R., *Ozone in Water Treatment: Application and Engineering*. Lewis Publishers: USA, 1991.

13. Alder, M. G.; Hill, G. R., The kinetics and mechanism of hydroxide ion catalyzed ozone decomposition in aqueous solution. *J. Am. Chem. Soc.* **1950,** *72* (5), 1884-1886.

14. Kilpatrick, M. L.; Herrick, C. C.; Kilpatrick, M., The decomposition of ozone in aqueous solution. *J. Am. Chem. Soc.* **1956,** *78* (9), 1784-1789.

15. Buhler, R. E.; Staehlin, J.; Hoigné, J., Ozone decomposition in water studied by pulse radiolysis 1. HO_2 / O_2^- and HO_3 / O_3^- as intermediates. *J. Phys. Chem.* **1984,** *88* (12), 2560-2564.

16. Staehelin, J.; Buhler, R. E.; Hoigné, J., Ozone decomposition in water studied by pulse radiolysis 2. OH and HO_4 · as chain intermediates. *J. Phys. Chem.* **1984,** *88* (24), 5999-6004.

17. Forni, L.; Bohnemann, D.; Hart, E. J., Mechanism of the hydroxide ion initiated decomposition of ozone in aqueous solution. *J. Phys. Chem.* **1982,** *86*, 255-259.

18. Hoigné, J.; Bader, H., Ozonation of water: Selectivity and rate of oxidation of solutes. *Ozone Sci. Eng.* **1979,** *1*, 73-85.

19. Hoigné, J.; Bader, H., Rate constants of reactions of ozone with organic and inorganic compounds in water - I Non-Dissociating Organic Compounds. *Water Res.* **1983,** *17*, 173-183.

20. Simic, M.; Neta, P.; Hayon, E., Pulse radiolysis study of alcohols in aqueous solution. *J. Phys. Chem.* **1969,** *73* (11), 3794-3800.

21. Willson, R. L.; Greenstock, C. L.; Adams, G. E.; Wageman, R.; Dorfman, L. M., The standardization of hydroxyl radical rate data from radiation chemistry. *Int. J. Radiat. Phys. Ch.* **1971,** *3* (3), 211-220.

22. Haag, W. R.; Yao, C. C. D., Rate constants for reaction of hydroxyl radicals with several drinking water contaminants. *Environ. Sci. Technol.* **1992,** *26*, 1005-1013.

23. Buxton, G. V.; Greenstock, C. L.; Helman, W. P.; Ross, A. B., Critical review of rate constant for reactions of hydrated electrons, hydrogen atoms and hydroxyl radicals in aqueous solution. *J. Phys. Chem. Ref. Data* **1988,** *17* (2), 51-886.

24. Hoigné, J.; Bader, H., The role of hydroxyl radical reactions in ozonation processes in aqueous solutions. *Water Res.* **1976,** *10*, 377-386.

25. Hoigné, J.; Bader, H., Ozonation of Water: Role of hydroxyl radical as oxidizing intermediates. *Science* **1975,** *190*, 782-783.

26. Staehelin, J.; Hoigné, J., Decomposition of ozone in water in the presence of organic solutes acting as promoters and inhibitors of radical chain reactions. *Environ. Sci. Technol.* **1985,** *19* (12), 1206-1213.

27. Elovitz, M.; von Gunten, U., Hydroxyl radical/ozone ratio during ozonation process I. The R_{ct} Concept. *Ozone Sci. Eng.* **1999,** *21*, 239-260.

28. Westerhoff, P.; Song, R.; Amy, G. L.; Minear, R., Applications of ozone decomposition models. *Ozone Sci. Eng.* **1997,** *19* (1), 55-73.

29. von Gunten, U., Ozonation of drinking water: Part I. Oxidation kinetics and product formation. *Water Res.* **2003,** *37* (7), 1443-1467.

30. Pi, Y.; Schumacher, J.; Jekel, M., The use of *para*-chlorobenzoic acid (pCBA) as an ozone/hydroxyl radical probe compound. *Ozone Sci. Eng.* **2005,** *27*, 431-436.

31. Vanderford, B. J.; Rosario-Ortiz, F. L.; Snyder, S. A., Analysis of *p*-chlorobenzoic acid in water by liquid-chromatography-tandem mass spectrometry. *J. Chromatogr. A* **2007,** *1164*, 219-223.

32. Acero, J. L.; von Gunten, U., Characterization of oxidation processes: Ozonation and the AOP O_3/H_2O_2. *J. Am. Water Works Ass.* **2001,** *93* (10), 90-100.

33. Yao, C. C. D.; Haag, W. R., Rate constants for direct reactions of ozone with several drinking water contaminants. *Water Res.* **1991,** *25* (7), 761-773.

34. Neta, P.; Dorfman, L. M., Pulse radiolysis studies. XIII: Rate constants for the reaction of hydroxyl radicals with aromatic compounds in aqueous solutions. *Adv. Chem. Ser.* **1968,** *81*, 222-230.

35. Buffle, M. O.; Schumacher, J.; Salhi, E.; Jekel, M.; von Gunten, U., Measurement of the initial phase of ozone decomposition in water and wastewater by means of a continuous quench-flow system: Application to disinfection and pharmaceutical oxidation. *Water Res.* **2006,** *40* (9), 1884-1894.

36. Elovitz, M.; Von Gunten, U.; Kaiser, H. P., Hydroxyl radical/ozone ratio during ozonation processes. II The effect of temperature, pH, alkalinity and DOM properties. *Ozone Sci. Eng.* **2000,** *22*, 123-150.

37. Buffle, M. O.; von Gunten, U., Phenols and amine induced OH generation during the initial phase of natural water ozonation. *Environ. Sci. Technol.* **2006,** *40* (9), 3057-3063.

38. Letterman, R. D., *Water Quality and Treatment: A Handbook of Community Water Supplies*. 5th ed.; McGraw-Hill: United States of America, 1999.

39. Crittenden, J. C.; Trussell, R. R.; Hand, D. W.; Howe, K. J.; Tchobanoglous, G., *Water Treatment: Principles and Design*. 2nd ed.; John Wiley & Sons: United States of America, 2005.

40. Benjamin, M. M., *Water Chemistry*. McGraw-Hill: Singapore, 2002.

41. Thurman, E. M., *Organic geochemistry of natural waters*. Martinus Nijhof/Dr W. Junk: Dordrecht, 1985.

42. Leenheer, J. A., Comprehensive approach to preparative isolation and fractionation of dissolved organic carbon from natural waters and wastewaters. *Environ. Sci. Technol.* **1981,** *15* (5), 578-587.

43. Thurman, E. M.; Malcolm, R. L., Preparative Isolation of Aquatic Humic Substances. *Environ. Sci. Technol.* **1981,** *15* (4), 463-466.

44. Aiken, G. R.; Mcknight, D. M.; Thorn, K. A.; Thurman, E. M., Isolation of hydrophilic organic acids from water using nonionic macroporous resins. *Org. Geochem.* **1992,** *18* (4), 567-573.

45. Mantoura, R. F. C.; Riley, J. P., Analytical concentration of humic substances from natural waters. *Anal. Chim. Acta* **1975,** *76* (1), 97-106.

46. Thurman, E. M.; Malcolm, R. L.; Aiken, G. R., Prediction of capacity factors for aqueous organic solutes adsorbed on a porous acrylic resin. *Anal. Chem.* **1978,** *50* (6), 775-779.

47. Aiken, G. R.; Thurman, E. M.; Malcolm, R. L., Comparison of XAD macroporous resins for the concentration of fulvic acid from aqueous solution. *Anal. Chem.* **1979,** *51* (11), 1799-1803.

48. Krasner, S. W.; Croue, J. P.; Buffle, J.; Perdue, E. M., Three approaches for characterizing NOM. *J. Am. Water Works Ass.* **1996,** *88* (6), 66-79.

49. Leenheer, J. A.; Croue, J. P., Characterizing Dissolved Aquatic Organic Matter. *Environ. Sci. Technol.* **2003,** *37* (1), 18-26.

50. Reckhow, D. A.; Singer, P. C.; Malcolm, R. L., Chlorination of humic materials: Byproduct formation and chemical interpretations. *Environ. Sci. Technol.* **1990,** *24*, 1655-1664.

51. Thurman, E. M.; Wershaw, R. L.; Malcolm, R. L.; Pinckney, D. J., Molecular size of aquatic humic substances. *Org. Geochem.* **1982,** *4*, 27-35.

52. Marhaba, T. F.; Van, D.; Lippincott, R. L., Changes in NOM fractionation through treatment: A comparison of ozonation and chlorination. *Ozone Sci. Eng.* **2000,** *22*, 249-266.

53. Ma, H.; Allen, H. E.; Yin, Y., Characterization of isolated fractions of dissolved organic matter from natural waters and a wastewater effluent. *Water Res.* **2001,** *35* (4), 985-996.

54. Kim, M. H.; Yu, M. J., Characterization of NOM in the Han River and Evaluation of treatability using UF-NF membrane. *Environ. Res.* **2005,** *97*, 116-123.

55. Kim, H. C.; Yu, M. J., Characterization of natural organic matter in conventional water treatment processes for selection of treatment processes focused on DBPs control. *Water Res.* **2005,** *39*, 4779-4789.

56. Swietlik, J.; Dabrowska, A.; Raczyk-Stanislawiak, U.; Nawrocki, J., Reactivity of natural organic matter fractions with chlorine dioxide and ozone. *Water Res.* **2004,** *38*, 547-558.

57. Sposito, G., *The Chemistry of Soil*. Oxford University Press: United States of America, 1989.

58. Pomes, M. L.; Green, W. R.; Thurman, E. M.; Orem, W. H.; Lerch, H. E., DBP formation potential of aquatic humic substances. *J. Am. Water Works Ass.* **1999,** *91* (3), 103-115.

59. Amy, G. L., Fundamental understanding of organic matter fouling of membranes. *Desalination* **2008,** *231*, 44-51.

60. Lee, N.; Amy, G. L.; Croue, J. P., Low-pressure membrane (MF/UF) fouling associated with allochthonous versus autochthonous natural organic matter. *Water Res.* **2006,** *40*, 2357-2368.

61. Siddiqui, M. S.; Amy, G. L.; Murphy, B. D., Ozone enhanced removal of natural organic matter from drinking water sources. *Water Res.* **1997,** *31* (12), 3098-3106.

62. Westerhoff, P.; Aiken, G. R.; Amy, G. L.; Debroux, J., Relationships between the structure of natural organic matter and its reactivity towards molecular ozone and hydroxyl radicals. *Water Res.* **1999,** *33* (10), 2265-2276.

63. Feng, X.; Legube, B., Enhancement of radical chain reactions of ozone in water in the presence of an aquatic fulvic acid. *Ozone Sci. Eng.* **1991,** *13* (3), 349-363.

64. Halling-Sorensen, B.; Nors Nielsen, S.; Lanzky, P. F.; Ingerslev, F.; Holten Lutzhoft, H. C.; Jorgensen, S. E., Occurrence, fate and effects of pharmaceutical substances in the environment - A Review. *Chemosphere* **1998,** *36* (2), 357-393.

65. Zuccato, E., Castiglioni, S., Fanelli, R., bagnati, R. and Calamari, D., *Pharmaceuticals in the environment: Changes in the presence and concentrations of pharmaceuticals for human use in Italy*. 2nd ed.; Springer: Germany, 2004.

66. Metcalfe, C.; Miao, X. S.; Hua, W.; Letcher, R.; Servos, M., *Pharmaceuticals in the Canadian environment*. Springer: Germany, 2004.

67. Ternes, T. A., Occurrence of drugs in German sewage treatment plants and rivers. *Water Res.* **1998,** *32* (11), 3245-3260.

68. Yoon, Y.; Ryu, J.; Choi, B.-G.; Snyder, S. A., Occurrence of endocrine disrupting compounds, pharmaceuticals and personal care products in the Han River (Seoul, Korea). *Sci. Total Environ.* **2010,** *408*, 636-643.

69. Lin, A. Y.-C.; Yu, T.-H.; Lin, C.-F., Pharmaceutical contamination in residential, industrial, and agricultural waste streams: Risk to aqueous environments in Taiwan. *Chemosphere* **2008,** *74*, 131-141.

70. Kim, S., D.; Cho, J.; Kim, I. S.; Vanderford, B. J.; Snyder, S. A., Occurrence and removal of pharmaceuticals and endocrine disruptors in South Korean surface, drinking, and wastewaters. *Water Res.* **2007,** *41*, 1013-1021.

71. Castiglioni, S.; Bagnati, R.; Fanelli, R.; Pomati, F.; Calamari, D.; Zuccato, E., Removal of pharmaceuticals in sewage treatment plants in Italy. *Environ. Sci. Technol.* **2006,** *40*, 357-363.

72. Peng, X.; Yu, Y.; Tang, C.; Tan, J.; Huang, Q.; Wang, Z., Occurrence of steroid estrogens, endocrine-disrupting phenols, and acid pharmaceutical residues in urban riverine water of the Pearl River Delta, South China. *Sci. Total Environ.* **2008,** *397*, 158-166.

73. Kolpin, D. W.; Furlong, E. T.; Meyer, M. T.; Thurman, E. M.; Zaugg, S. D.; Barber, L. B.; Buxton, H. T., Pharmaceuticals, hormones, and other organic wastewater contaminants in US streams, 1999-2000: A national reconnaissance. *Environ. Sci. Technol.* **2002,** *36* (6), 1202-1211.

74. Ternes, T. A.; Meisenheimer, M.; McDowell, D.; Sacher, F.; Brauch, H. J.; Gulde, B. H.; Preuss, G.; Wilme, U.; Seibert, N. Z., Removal of pharmaceuticals during drinking water treatment. *Environ. Sci. Technol.* **2002,** *36* (17), 3855-3863.

75. Sohn, J.; Amy, G. L.; Yoon, Y., Process-train profiles of NOM through drinking water treatment plant. *J. Am. Water Works Ass.* **2007,** *99* (6), 145-153.

76. Zwiener, C.; Frimmel, F. H., Oxidative treatment of pharmaceuticals in water. *Water Res.* **2000,** *34* (6), 1881-1885.

77. Huber, M. M.; Canonica, S.; Park, G. Y.; von Gunten, U., Oxidation of pharmaceuticals during ozonation and advanced oxidation processes. *Environ. Sci. Technol.* **2003,** *37* (5), 1016-1024.

78. Westerhoff, P.; Yoon, Y.; Snyder, S.; Wert, E., Fate of endocrine-disruptor, pharmaceutical, and personal care product chemicals during simulated drinking water treatment processes. *Environ. Sci. Technol.* **2005,** *39* (17), 6649-6663.

79. Snyder, S. A.; Wert, E. C.; Rexing, D. J.; Zegers, R. E.; Drury, D. D., Ozone oxidation of endocrine disruptors and pharmaceuticals in surface water and wastewater. *Ozone Sci. Eng.* **2006,** *28* (6), 445-460.

80. APHA; WWA; WEF, *Standard Methods For The Examination of Water and Wastewater*, 21st Ed. In APHA: Washington, DC, 2005.

81. Hoigné, J.; Bader, H., Characterization of water quality criteria for ozonation processes. Part II: Lifetime of added ozone. *Ozone Sci. Eng.* **1994,** *16*, 121-134.

82. Staehelin, J.; Hoigné, J., Decomposition of ozone in water: Rate of initiation by hydroxide ions and hydrogen peroxide. *Environ. Sci. Technol.* **1982,** *16* (10), 676-681.

83. Hoigné, J.; Bader, H., Rate constants of reactions of ozone with organic and inorganic compounds in water - II Dissociating organic compounds. *Water Res.* **1983,** *17*, 185-194.

84. Bader, H.; Hoigné, J., Determination of ozone in water by the indigo method. *Water Res.* **1981,** *15*, 449-456.

85. Bezbarua, B. K.; Reckhow, D. A., Modification of the standard neutral ozone decomposition model. *Ozone Sci. Eng.* **2004,** *26*, 345-357.

86. Schuchmann, M. N.; von Sonntag, C., Hydroxyl radical-induced oxidation of 2-methyl-2-propanol in oxygenated aqueous solution. A product and pulse radiolysis study. *J. Phys. Chem.* **1979,** *83* (7), 780-784.

87. Adams, G. E.; Boag, J. W.; Currant, J.; Michael, B. D., Absolute rate constants for the reaction of the hydroxyl radical with organic compounds. In *Pulse Radiolysis*, Ebert, M.; Keene, J. P.; Swallow, A. J.; Baxendale, J. H., Eds. Academic Press: New York, 1965.

88. Elovitz, M.; von Gunten, U.; Kaiser, H. P., The influence if dissolved organic matter character on ozone decomposition rates and R_{ct}. *ACS Sym. Ser.* **2000**, *761*, 248-269.

89. Bailey, P. S., The reactions of ozone with organic compounds. *Chem. Rev.* **1958,** *58* (5), 925-1010.

90. Westerhoff, P.; Mezyk, S. P.; Cooper, W. J.; Minakata, D., Electron pulse radiolysis determination of hydroxyl radical rate constants with Suwannee River fulvic acid and other dissolved organic matter isolates. *Environ. Sci. Technol.* **2007,** *41* (13), 4640-4646.

91. Rosario-Ortiz, F. L.; Mezyk, S. P.; Doud, D. F. R.; Snyder, S. A., Quantitative correlation of absolute hydroxyl radical rate constants with non-isolated effluent organic matter bulk properties in water. *Environ. Sci. Technol.* **2008,** *42* (16), 5924-5930.

92. McKay, G.; Dong, M. M.; Kleinman, J. L.; Mezyk, S. P.; Rosario-Ortiz, F. L., Temperature dependence of the reaction between the hydroxyl radical and organic matter. *Environ. Sci. Technol.* **2011,** *45* (16), 6932-6937.

93. Hoigné, J.; Bader, H.; Haag, W. R.; Staehelin, J., Rate constants of reactions of ozone with organic and inorganic compounds in water - III Inorganic compounds and radicals. *Water Res.* **1985,** *19*, 993-1004.

94. Lin, Y. P.; Singer, P. C.; Aiken, G. R., Inhibition of calcite precipitation by natural organic material: Kinetics, mechanism, and thermodynamics. *Environ. Sci. Technol.* **2005,** *39* (17), 6420-6428.

95. Ashton, D.; Hilton, M., Thomas, K.D., Investigating the environmental transport of human pharmaceuticals to streams in the United Kingdom. *Sci. Total Environ.* **2004,** *333*, 164-184.

96. Knepper, T. P.; Werner A.; Bogenschütz, G., Determination of synthetic chelating agents in surface and wastewater by ion chromatography-mass spectrometry. *J Chroma. A*, **2005**, *1085*, 240-246.

97. Stemmler, K.; Glod, G.; von Gunten, U., Oxidation of metal-diethylenetriamine-pentaacetate (DTPA) - Complexes during drinking water ozonation. *Water Res.* **2001,** *35* (8), 1877-1886.

98. Dodd, M. C.; Buffle, M. O.; von Gunten, U., Oxidation of antibacterial molecules by aqueous ozone: Moiety-specific reaction kinetics and application to ozone-based wastewater treatment. *Environ. Sci. Technol.* **2006,** *40* (6), 1969-1977.

99. Benitez, F. J.; Acero, J. L.; Real, F. J.; Roldan, G., Ozonation of pharmaceutical compounds: Rate constants and elimination in various water matrices. *Chemosphere* **2009,** *77* (1), 53-59.

100. Song, W.; Cooper, W. J.; Mezyk, S. P.; Greaves, J.; Peake, B. M., Free radical destruction of beta-blockers in aqueous solution. *Environ. Sci. Technol.* **2008,** *42*, (4) 1256-1261.